BULLETIN OF THE EARTHQUAKE
RESEARCH INSTITUTE
UNIVERSITY OF TOKYO
Vol. 64 (1989), pp. 391-431

Geology of Sagami Bay and its Environs

—Reports on the Results of KT88-1 Cruise—

Kantaro FUJIOKA[1], Masataka KINOSHITA[2], Wonn SOH[1], Shinji TSUKAWAKI[1] Juichiro ASHI[1], Kazumi AKIMOTO[2] and Masaharu WATANABE[1]

[1] Ocean Research Institute, University of Tokyo
[2] Earthquake Research Institute, University of Tokyo

(Received July 3, 1989)

Abstract

Geological and geophysical characteristics of Sagami Bay, 80 km west off Tokyo, were studied on KT88-1 cruise by R/V Tansei-Maru, Ocean Research Institute, University of Tokyo, February 1988. In this paper, we summarized the results of the geological and geophysical studies, and discussed two topics: 1) The Hatsushima deep-sea community which is one of the largest communities around the Japanese Islands is located in the western part of the Sagami Trough. Heat flow anomalies up to 1,680 mW/m^2 and high methane anomalies of the surrounding seawater were discovered there. We deduce that the deep sea community has most likely originanted and is developed by submarine hot springs related to magmatic activity. 2) Pebbly mudstones including various sizes and kinds of volcanic materials were obtained by dredge hauls at several sites of the Okinoyama Bank Chain. No *in-situ* volcanic material was obtained. The magnetic anomalies along the Okinoyama Bank Chain give no evidence of volcanic seamounts. We believe that the Okinoyama Bank Chain is not underlain by volcanic seamounts, but rather by large blocks of accreted sediments, including large amounts of volcaniclastic materials deposited in the forearc basins of the Izu-Bonin Ridge near the volcanic front. The mutual relation between the Sagami Trough and the Bank Chain should be similar to the relation between the So-o Trough and the southern offshore Boso area.

Contents

1. Introduction

Sagami Bay is located at the plate boundary between the Philippine Sea Plate and the Northeast Japan (North America) Plate (Fig. 1a). The Bay is tectonically one of the most active areas in the world, where the Great Kanto Earthquake took place in 1923 (KANAMORI, 1971). The Sagami Trough runs from north to south or NNW to SSE in the central part of the Sagami Bay and continues to the So-o Trough at the east of Oshima island where the trend of the So-o Trough is almost west to east (FUJIOKA *et al.*, 1984). Sagami Bay can be classified morphologically into three areas; the western, central and eastern areas. Figures 1a and 1b show an overview of the topographic features of Sagami Bay with station survey points. Table 1 shows the station survey log of the cruise.

The western area is situated on the Philippine Sea Plate covered with mostly Quaternary submarine volcanoes, where irregularly and conically shaped topographies are well-developed. The central area is mostly occupied by the axial deep water channel of Sagemi Trough. Tokyo submarine fan occupies the main part of the central area, which is connected to the Tokyo deep sea canyon. The Sagami Trough is valley-shaped, and is filled with thick coarse-grained detritus derived from the Izu-Bonin Arc as well as from the Honshu Arc. The eastern area is dominated by topographic highs called the Okinoyama Bank Chain. The top of the Okinoyama Bank Chain, which is shallower than 500 meters, has a flat surface eroded by wave action during low sea level stands.

As for the origin and development of the Sagami Bay, many interpretations have been presented (KAGAMI *et al.*, 1986; SUGIMURA, 1972; KIMURA, 1976). For example, the Okinoyama Bank Chain and its adjacent topographic highs have been thought to be a chain of submarine volcanoes which supplied volcaniclastic materials to the Miura and Boso Peninsulas during the Mio-Pliocene age (KIMURA, 1976; MATSUDA, 1962). Recently, a deep-sea animal community was found in the western part of the Bay, east off the Izu Peninsula, during dives with the deep-sea submersible "Shinkai 2000" of JAMSTEC (OHTA, *et al.*, 1987; FUJIOKA and TAIRA, 1989; HASHIMOTO *et al.*, in press).

During the cruise of R/V Tansei-Maru, Ocean Research Institute,

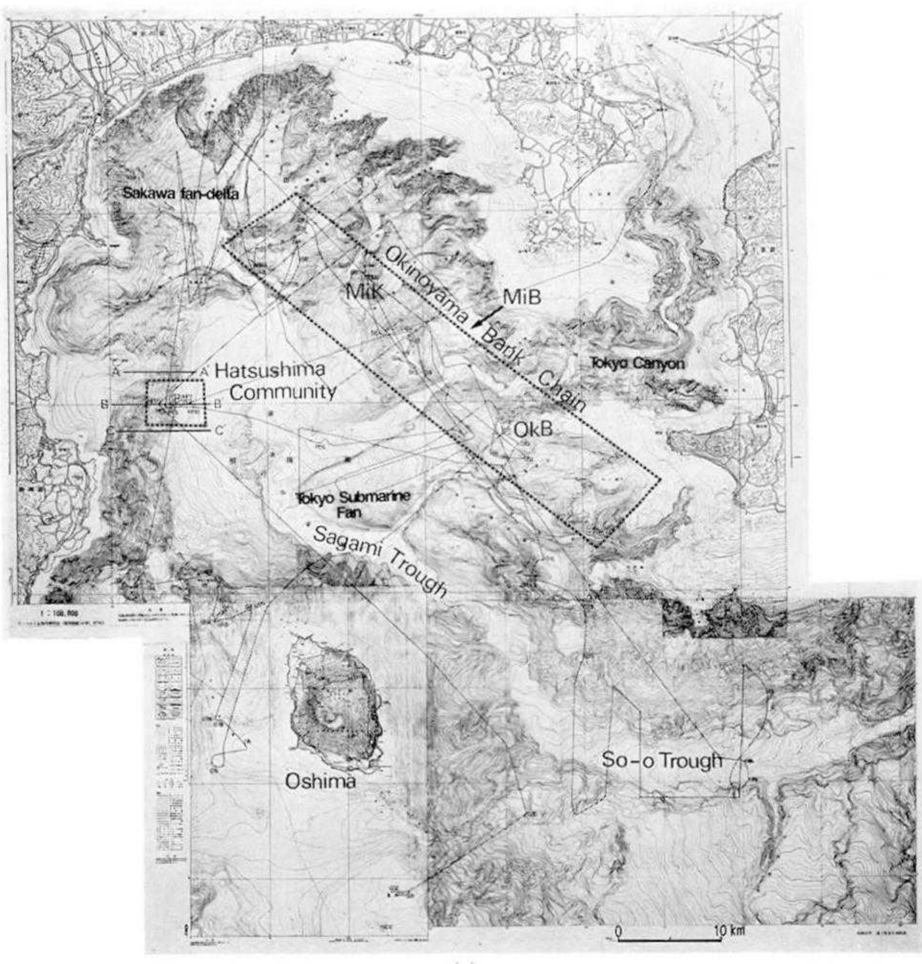

(a)

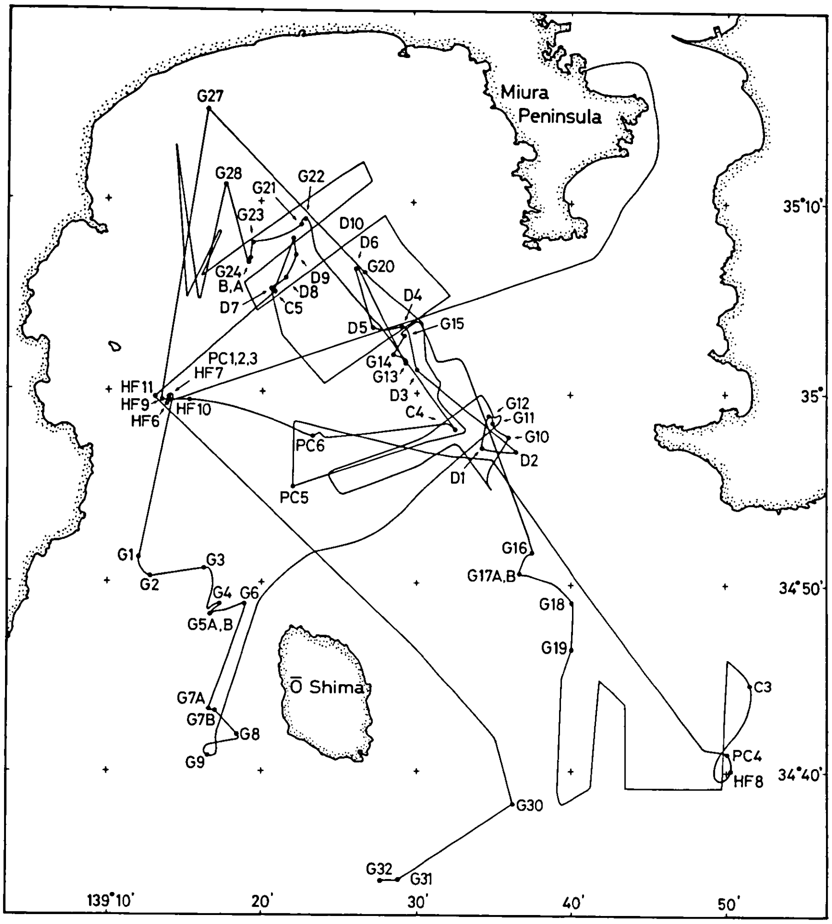

(b)

Fig. 1. Topographic overview of Sagami Bay showing the (a) topographic characteristics of the Sagami Bay and (b) sampling positions of KT88-1 cruise. G: grab, D: dredge, PC: piston core, C: deep-sea camera, and HF: heat flow. Square surrounded by broken lines in (a) shows the location of the Hatsushima Community. OkB: Okinoyama Bank, MiK: Miura Knoll, MiB: Miura Basin.

University of Tokyo, we had the opportunity to survey across Sagami Bay, the Hatsushima community, the central portion of Sagami Trough and the Okinoyama Bank Chain, and obtained important information on the origin of the deep-sea community and Okinoyama Bank Chain. We summarize here the results of the cruise, and present new insight on the origin of the Hatsushima community and the Okinoyama Bank Chain.

Table 1. Station log of KT88-1 cruise in Sagami Bay. Time (S): Time start; Time (H): Time hit bottom, Time (L): Time leave bottom; Time (F); Time finished.

No.	Drive	Date	Time (S)	Time (H)	Time (L)	Time (F)	Latitude (N)	Longitude (E)	Depth(m)	Remarks
1	HF-6	2/18	09:58	10:36	10:48	11:04	34°59.7′	139°13.9′	1233	Hatsushima Community
2	PC-1		11:15	11:42		12:02	59.96	13.89	1220	No Recovery
3	PC-2		12:14	12:33		13:08	35°00.0	14.2	1281	
4	HF-7		13:27	13:57	14:15	14:28	34°59.9	14.2	—	
5	PC-3		14:50	15:14		15:28	35°00.0	14.0	1251	Calyptogena
6	G-1		16:53	16:53			34°51.5	12.0	1029	
7	G-2		17:35	17:52		18:08	34°50.588	12.7	1000	
8	G-3		18:57	19:10		19:22	50.9	16.4	645	Nishichigasaki Knoll
9	G-4		19:53	20:07		20:20	49.0	17.1	702	
10	G-5A		20:41	20:57			48.5	16.6	652	
11	G-5B		21:07	21:20	21:22	21:32	48.7	16.8	713	Senba Kholl
12	G-6		21:56	22:06		22:15	49.0	18.9	467	
13	G-7A		23:09	23:14		23:18	43.4	16.6	193	
14	G-7B		23:23	23:27		23:32	43.3	16.9	186	
15	G-8		23:53	23:56		23:59	42.0	18.5	142	
16	G-9	2/19	00:25	00:30			41.0	16.6	270	Senda Spur
17	G-10		06:39	06:45			57.8	35.9	89	Okinoyama
18	G-11		07:08	07:09		07:10	58.4	34.9	76	
19	G-12		07:20	07:25		07:27	59.0	34.8	82	
20	D-1		08:10	08:17	08:40	08:47	57.4	34.2	202	Okinoyama
21	D-2		09:05	09:14	09.51	09.55	57.3	36.4	339	
22	D-3		10:47	11:01	11:53	12:03	35°01.4	30.1	581	Misaki Knoll
23	D-4		12:25	12:35	13:10	13:20	00.7	29.2	505	〃
24	D-5		13:37	13:50	14:24	14:40	03.7	27.4	822	〃
25	D-6		15:10	15.20	15:55	16:06	06.9	26.1	870	Miura Knoll
26	G-12		16:55	17:04		17:12	01.9	29.5	622	Misaki Knoll
27	G-14		17:32	17:39	17:40	17:46	02.3	28.6	537	〃
28	G-15		18:03	18:10		18:15	03.3	29.1	555	〃
29	G-16		20:00	20:10		20:16	34°51.7	37.5	490	Mera Spur
29	G-17A		20:37	20:50		21:03	50.6	36.6	721	
30	G-17B		21:14	21:29		21:40	50.6	36.7	682	

Table 1. (Continued)

No.	Drive	Date	Time (S)	Time (H)	Time (L)	Time (F)	Latitude (N)	Longitude (E)	Depth (m)	Remarks
31	G-18A		22:13	22:22			34°49.1′	139°39.8′	468	
32	G-18B		22:35	22:45			49.1	39.9	516	
33	G-19		23:20	23:35		23:46	46.7	39.9	690	
35	C-3	2/20	04:12	04:57	06:06	06:38	34°44.7	139°51.4	1917	
36	HF-8		07:40				40.2	50.4		So-o Trough
37	PC-4		09:48	10:24		10:55	41.1	50.2	2475	〃
38	PC-5		16:36	17:03		17:26	55.1	22.1	1578	Tokyo Submarine Fan
39	G-20		19:10	19:20		19:30	35°06.4	26.3	680	Miura Spur
40	G-27	2/21	07:25	07:26		07:28	15.1	16.4	95	Oiso Spur
41	HF-9		09:00	09:32	09:50	10:01	34°59.8	13.7		Hatsushima
42	HF-10		10:24	11:13	11:43	12:45	59.8	15.3	1329	〃
43	PC-6		12:46	13:10		13:32	57.9	23.3	1504	Tokyo Submarine Fan
44	C-4		14:30	14:39	16:01	16:06	58.2	32.7		Okinoyama
45	G-22		17:39	17:47		17:53	35°09.4	22.8	508	〃
46	G-21		18:07	18:13		18:19	09.2	22.8	479	Sagami Knoll
47	G-23		18:46	18:53		19:00	08.1	19.4	508	〃
48	G-24A		19:11	19:20		19:28	07.3	19.4	619	
49	G-24B		19:30	19:43		19:55	07.1	19.3	815	〃
50	G-28		20:33	20:49		21:02	11.1	17.9	880	
51	D-7	2/22	11:24	11:50	12:37	12:52	05.7	20.7	1111	Sagami Knoll
52	D-8		13:31	13:45	14:32	14:42	06.2	21.5	911	〃
53	D-9		15:13	15:25	16:05	16:15	07.5	22.2	760	〃
54	D-10		16:28	16:40	17:40	17:49	08.2	22.1	683	〃
55	C-5	2/22	18:27	18:59	20:18	20:33	35°05.7	139°20.8	1296	Sagami Knoll
56	HF-11		21:26	21:59	22:29	22:30	00.1	13.1		Hatsushima
57	G-30	2/23	01:07	01:28			34°38.4	36.3	1335	
58	G-31		02:37	02:38		02:40	34.2	28.8	84	Ohmurodashi
59	G-32A		02:49	02:51		02:52	34.1	27.9	86	〃
60	G-32B		02:55	02:57		02:58	34.1	27.8	86	〃

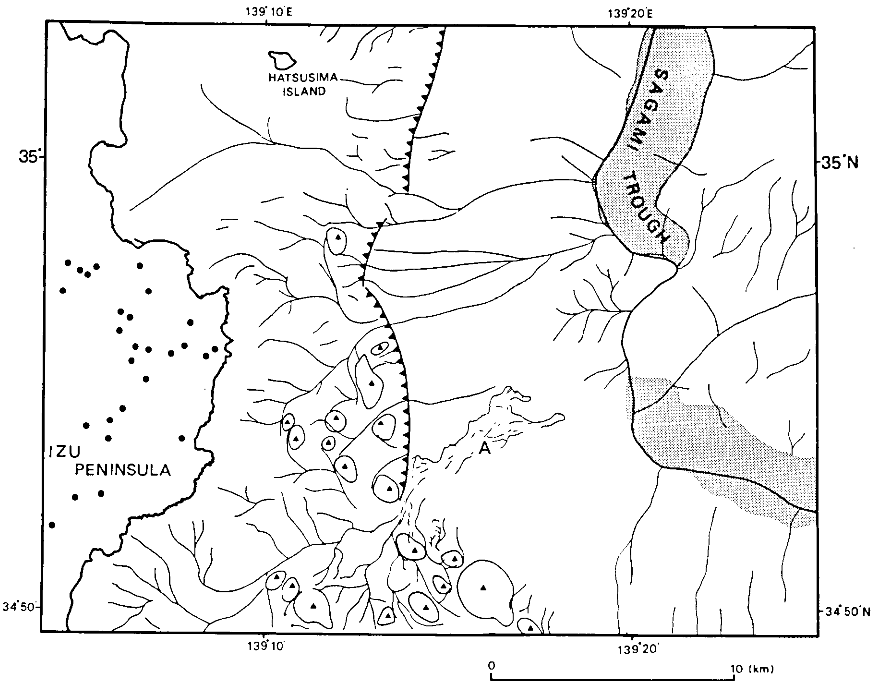

Fig. 2. Topographic features around the Hatsushima Community. ●: Higashi Izu monogenetic volcanoes. ▲: Higashi Izu-oki submarine volcanoes, -▲▲▲-: faults and inflexion line (modified from ISHIBASHI, 1976 and HAMURO *et al.*, 1980), A: Atagawa-oki submarine lava flow.

2. Hatsushima Area

2-1. Topography and geology

The Hatsushima community occupies the western part of Sagami Bay, just east of the Izu Peninsula, about 80 km west off Tokyo. Figure 2 shows the topographic features around this community. The eastern slope of the Izu Peninsula is rather steep as far as 1,100 meters in water depth, where the gradient abruptly changes along the distinct base of the slope. On the inflection line, the large communities consisting mostly of giant clams are found (OHTA *et al.*, 1987; HASHIMOTO *et al.*, 1989). Several conical active submarine volcanoes are situated just west of the inflection line (HAMURO *et al.*, 1980). Most submarine canyons on the steep slope continue farther down to the deeper part, but some canyons die out at the slope break. In the southwest corner of the map (Fig. 2), the flat topography of the submarine lava flow platform is identified ("A" in Fig. 2). This was found by the submersible "Shinkai 2000" and called "Atagawa-oki submarine lava flow" (NAKA, *et al.*, 1988;

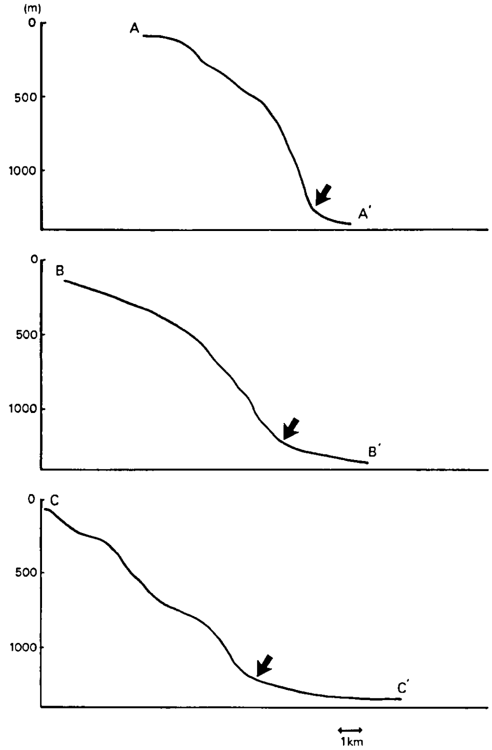

Fig. 3. West-east topographic cross sections of the Hatsushima Community. Positions of the cross section are shown in Fig. 1a. Arrows show the position of the active fault.

UI, *et al.*, 1988). Sediments covering the steep slope are volcanogenic sand and/or mud which include granules and pebbles of andesite and or basalt which are distributed onshore to the Izu Peninsula.

Figure 3 shows the west-east topographic cross sections across the community, showing a fault running along the inflection line near the community.

2-2. Size of the community

We tried to take deep sea photographs in order to evaluate the precise distribution of the community as well as the nature of the community. We successed in taking continuous photographs covering most of the area occupied by the community.

As shown in Figure 4, the community is approximately 4 m in length and about 2 m in width, and it consists mostly of bivalve *calyptogena* and crabs.

The community shows linear distribution along the 1,100 m depth contour, which is parallel to both the base of the slope of the east of Izu Peninsula and the general trend of the active faults in Figure 2, that is, northeast to southwest (ISHIBASHI, 1976; HAMURO *et al.*, 1980).

2-3. Nature of sediments

Surface sediments around the Hatsushima community were collected by grab sampler, piston corer and box corer. It is noteworthy that pyrites are commonly contained in the sediments, suggesting strong anoxic condition near the surface. Generally the surface sediments are rich in biogenic and volcanogenic materials.

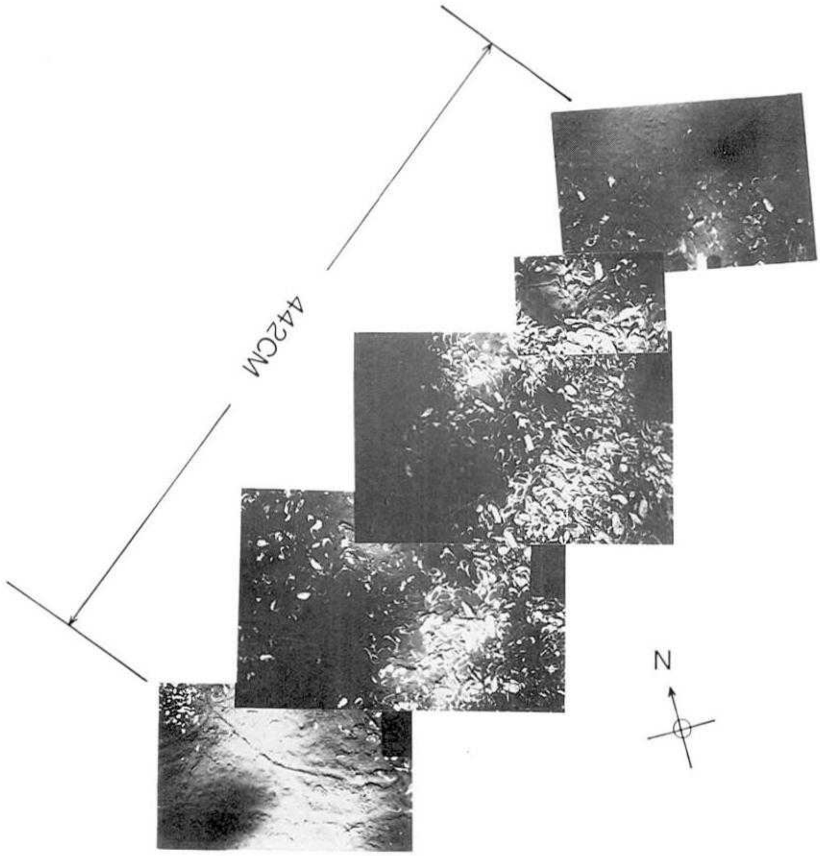

Fig. 4. Deep sea photograph showing the distribution of the Hatsushima Community.

Grab Samples: During the cruise, 32 grab sites were chosen to investigate the transportation and composition of sediments, and 24 samples were successfully obtained (Fig. 1b). In five samples (G-7, 10, 11, 31 and 32), coarse carbonate (limestone) fragments are found. Three samples (G-9, 18 and 19) are composed mainly of andesitic or basaltic coarse-grained sands and scoria. The G-24 sample consists of semi-consolidated siltstones.

Smear slide observations have been carried out on 15 grab samples which contain silt to fine sand sized grains (Table 2). All samples contain abundant biogenic components such as sponge spicules, calcareous nannofossils, foraminifers, diatoms and a small amount of silicoflagellata and radiolarians. Woody fragments are recognized in near-shore samples (G-22 and 28). There are few differences in mineral composition among these samples. In general, volcanogenic fragments predominate; broken glass shards with fragments of plagioclase are most abundant.

Table 2. Smear slide observations of surface sediments obtained during KT88-1 cruise.

Site	QTZ	PLG	HRN	OPX	CPX	GLS	PMC	DUS	SPO	NAN	FRM	RDS	DIA	SIL	PLT
G-1	8	20		2		30	5	15	6	6	6	2			
G-3	8	20		2	1	30	4	15	6	6	2		6		
G-4	5	10	2	2	1	20	2	5	10	10	10	5	10	5	
G-5	6	10		2		20	5	7	20	15	10	5			
G-6	6	17		2		20	5	10	20	10	10				
G-13	4	10		1		20	2	3	20	15	10		10	5	
G-14	10	20	2			30	13	5	5	5	5	2	3		
G-15	6	17		2		20	10	15	10	15	2		3		
G-16	8	25		2		35			10	10	2		5	3	
G-21	5	20	2			25	5	3	10	10	10		5	5	
G-22	6	20	2		2	25	3	2	10	10	5	3	5	5	2
G-23	5	15	1			15	4	10	10	10	10	5	10	5	
G-27	5	15	1			25	10	4	10	10	10		10		
G-28	5	15	1			25	10	4	10	10	10	3	5		2
G-30	9	20			1	30			10	8	7	7	5	3	

QTZ: quartz
PLG: plagioclase
HRN: hornblende
GLS: glass
PUM: pumice
DUS: dusty minerals

SPO: sponge
NAN: nannofossil
FRM: foraminifera
RAD: radiolaria
DIA: diatom
SIL: silicofragellata
PLT: plant

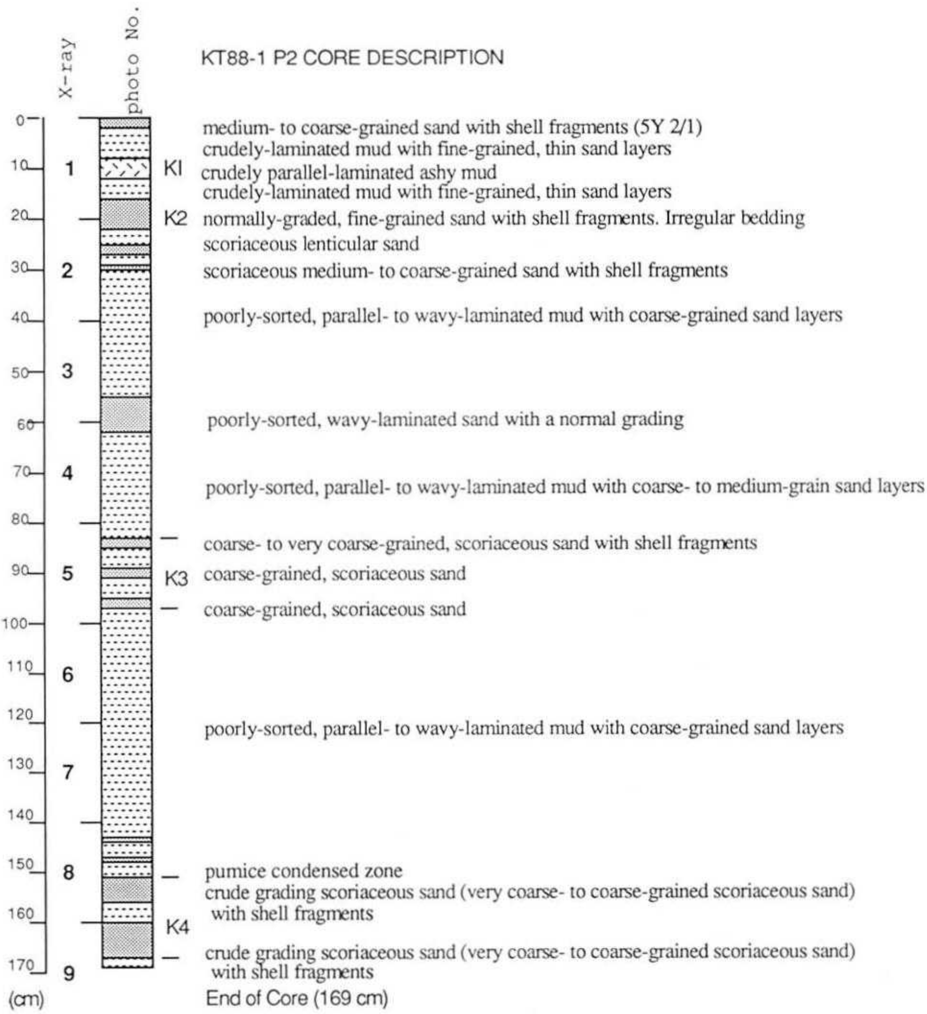

Fig. 5. Piston core log of the PC-2 obtained from the Hatsushima Community.

PC-2 and PC-3 Core Description: Upper portion (upper fan) of unnamed submarine cone about 4 km in diameter off Hatsushima

Two piston cores (PC-2 and PC-3) were successfully recovered near the Hatsushima community. Both piston cores are lithologically quite similar to each other. The following is the precise descriptions of the piston core (PC-2 and PC-3) samples.

PC-2 and PC-3 cores are composed entirely of alternations of fine- to coarse-grained sand and mud layers from top to bottom. The sand layer shows normal grading with sharp and smooth bed bases, and it

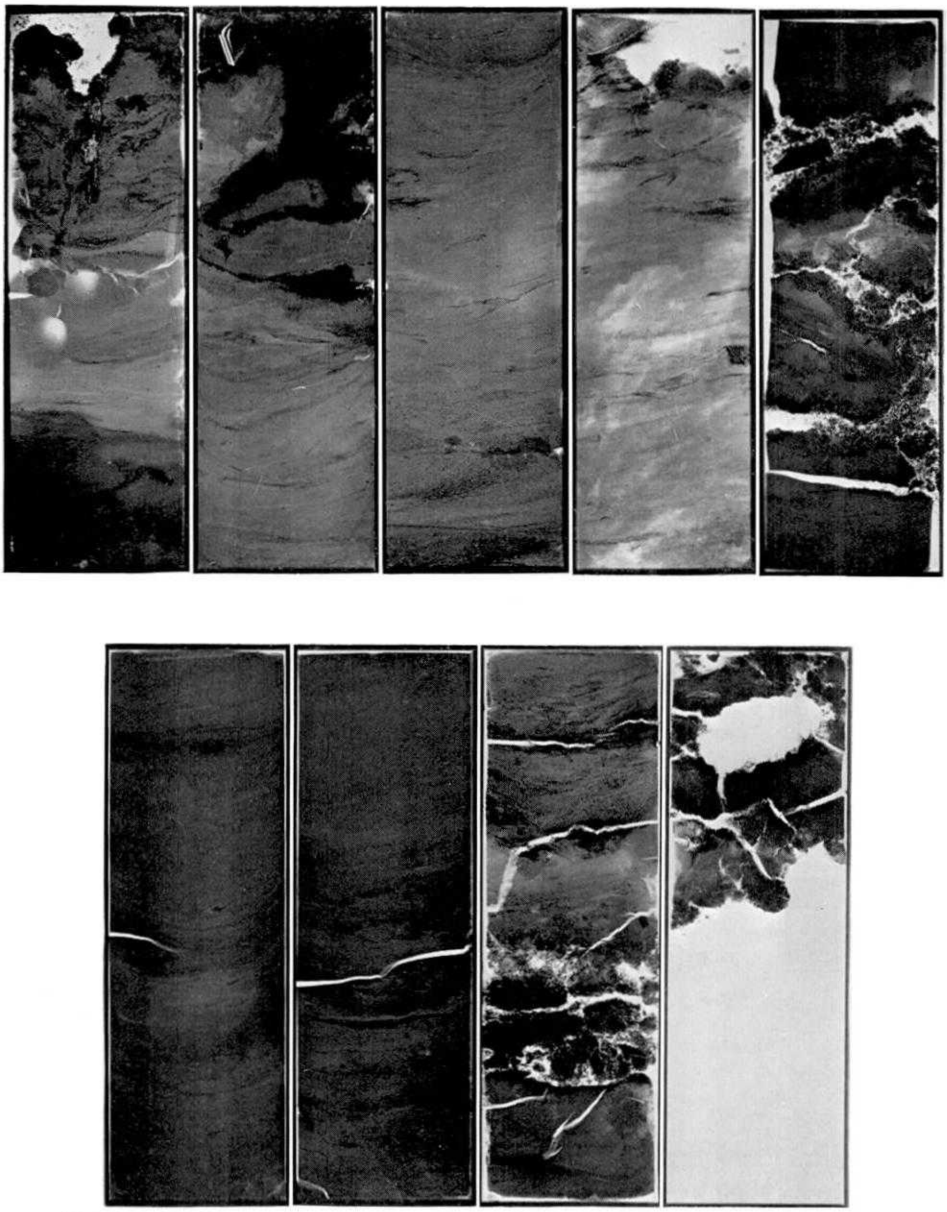

Fig. 6. Soft X-ray photographies of the PC-2 core sample (see Fig. 5). Vertical scale of each column is 20 cm showing top to bottom of the sediments from top left to bottom right in this figure.

is composed of volcaniclastic grains and molluscan shell fragments. The sand layers range from 2 cm to 8 cm in thickness. The sand layers can be divided into two types: the coarse-grained sand with shell

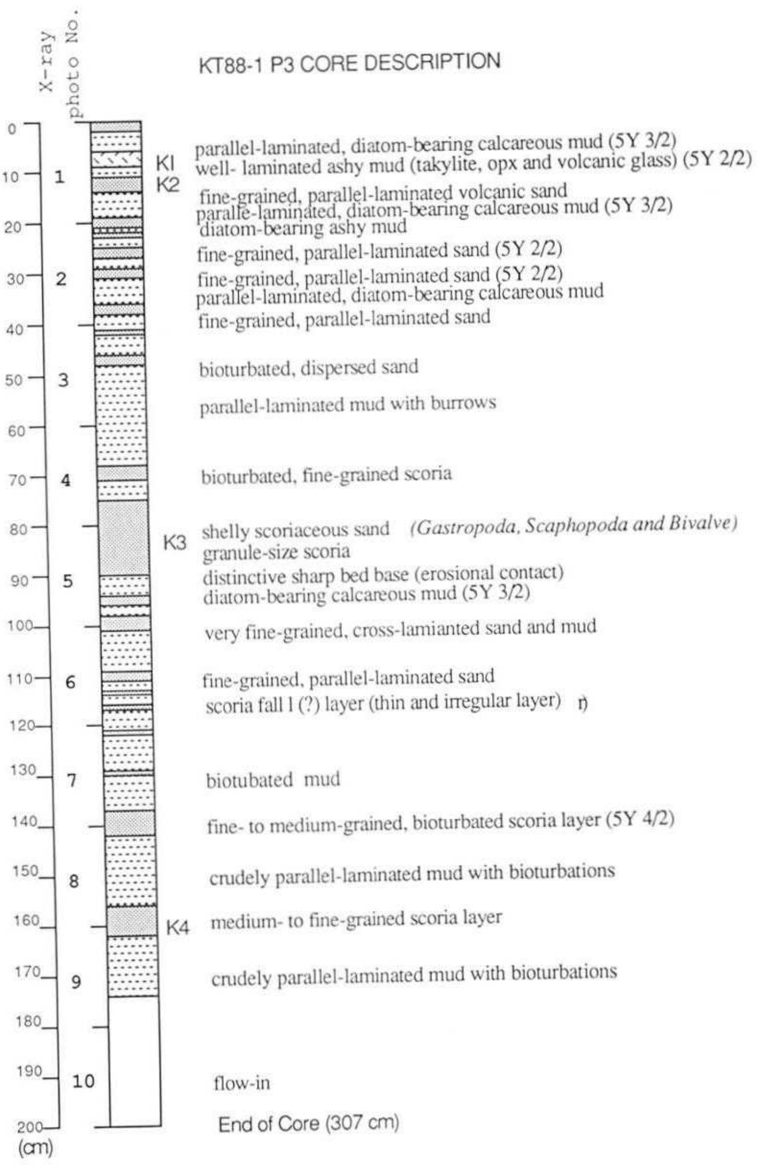

Fig. 7. Piston core log of the PC-3 obtained from the Hatsushima Community.

fragments and fine-grained, well-sorted sand. The former shows crude normal grading or structureless and it has a sharp and smooth bed base. It is composed chiefly of very coarse- to medium-grained scoria, consisting of fragments of well- to moderately-vesiculated volcanic glass with microlites of plagioclase and pyroxene, and shell fragments of gastropoda, scaphopoda and bivalves a few millimeters long. The

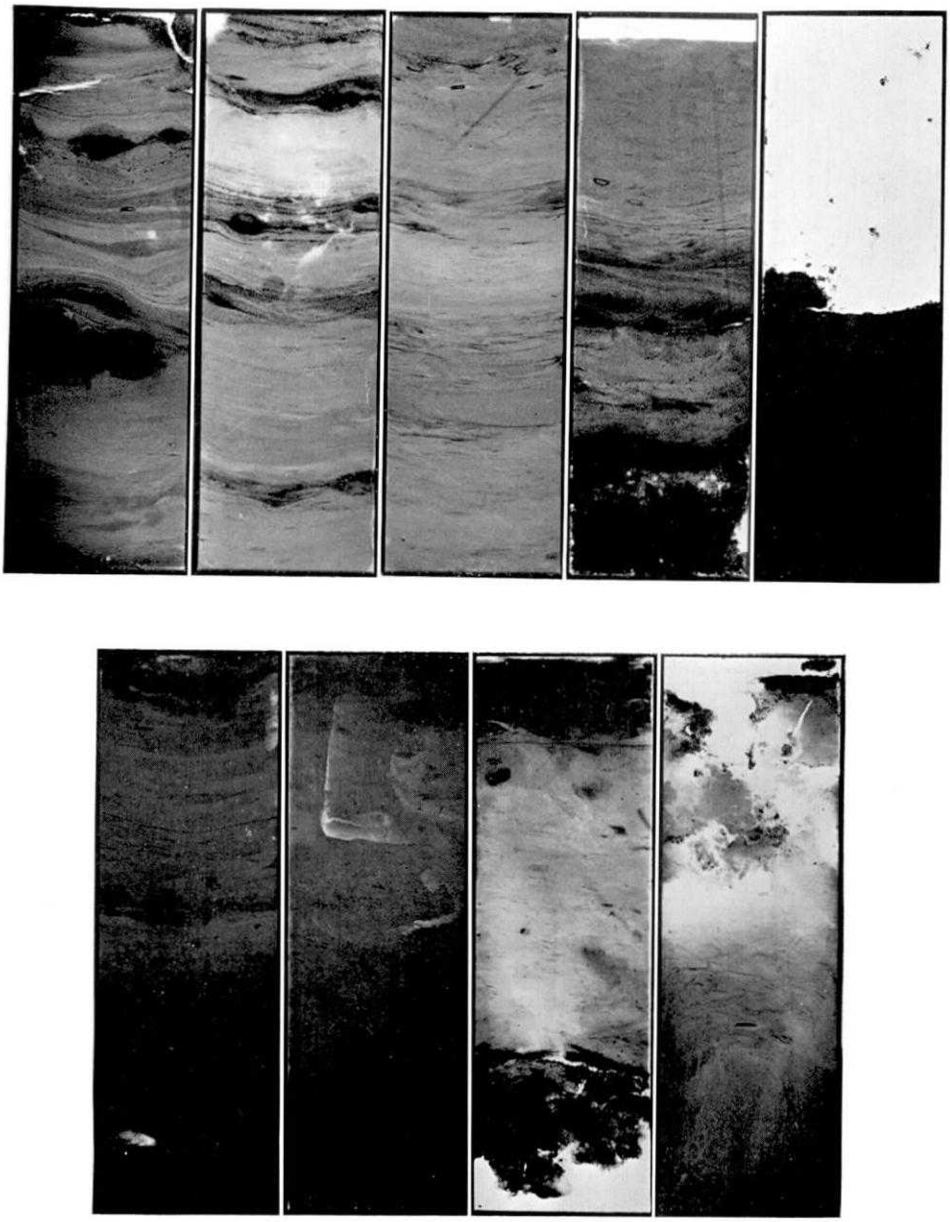

Fig. 8. Soft X-ray photographies of the PC-3 core sample (see Fig. 7). Scale is the same as Fig. 6.

latter is composed of muddy sand, and shows normal grading with poorly-defined top and base bed boundaries. It is composed mainly of volcanic glass of sideromelane, and fragmented crystals of plagioclase and pyroxene.

The mud, as the most dominant lithology of the core, shows parallel to wavy laminations, and is poorly sorted with scoria grains more than a few millimeters in diameter. The mud layers contain very thin lamina, less than a few millimeters thick, of fine- to coarse-grained sand. Under a smear slide, the mud consists mainly of clay, diatoms, sponge spicules and nannofossils. Small amounts of volcanic glass shards, foraminifers, silicoflagellates, and plagioclase grains are included. An ashy mud layer is identified between 3 cm and 9 cm below the top of the core (Figs. 5, 6, 7 and 8).

2-4. Heat flow measurement

During this cruise, nine heat flow measurements were performed off Hatsushima Island in the Sagami Bay (Figs. 1b and 9). Benthic communities of giant clams are found along the active fault trending NNE to SSW (Fig. 2), where temperature anomalies have been observed by the submersible 'Shinkai 2000' (OHTA *et al.*, 1987). Although it is very important to know the thermal features around this area, there exist almost no heat flow data so far (Fig. 9a). The heat flow was also measured at one site (HF-8 in Fig. 1b) located at the eastern end of Sagami Trough, south of the Boso Peninsula.

A temperature gradient was measured by penetrating a Bullard type marine geothermal probe

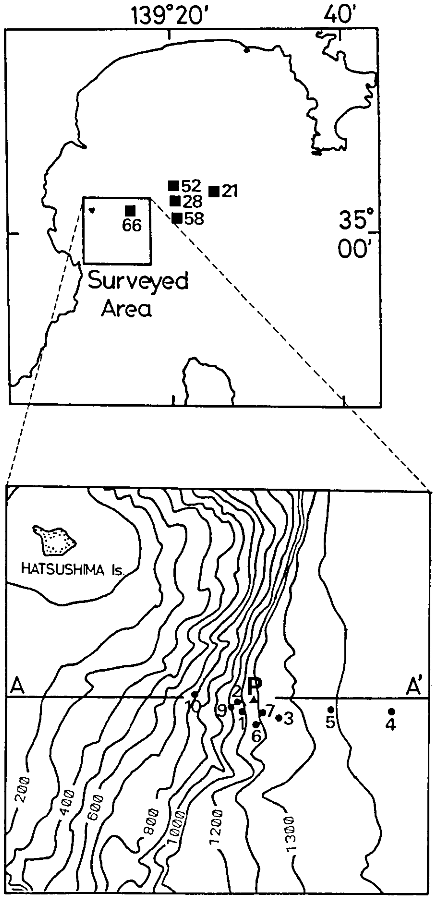

Fig. 9. (a) Heat flow data of the Sagami Bay obtained so far (mW/m²). (b) Heat flow stations during this cruise. P is the piston coring site PC-3 for the thermal conductivity measurement. A cross section will be taken along line A-A′ in Fig. 10.

Table 3. Heat flow stations and results.

Station	Latitude (N)	Longitude (E)	Depth (m)	PEN (m)	*N*	*G* (mK/m)	*K* (W/m/K)	*Q* (mW/m^2)
HF01	34°59.92′	139°13.80′	1200	1.0	3	539	0.79	425
HF02	34°59.99′	139°13.66′	1230	1.5	4	2130	0.79	1680
HF03	34°59.87′	139°14.46′	1285	2.5	6	201	0.79	159
HF04	34°59.92′	139°16.52′	1375	2.5	6	49	0.79	38
HF05	34°59.97′	139°15.46′	1362	2.5	6	73	0.79	58
HF06	34°59.71′	139°14.09′	1240	2.5	6	83	0.79	66
HF07	34°59.90′	139°14.19′	1260	2.5	6	210	0.79	166
HF08*	34°40.19′	139°50.40′	2454	fell				
HF09	34°59.81′	138°13.65′	1120	1.0	2	(260)	0.79	(205)
HF10	35°00.01′	139°13.06′	760	1.0	2	(69)	0.79	(54)
PC-3	35°00.0′	139°14.0′	1251	2.5			0.79±0.02	
PC-4*	34°41.1′	139°50.2′	2473	3.5			0.88±0.04	

Depth: the uncorrected water depth.
PEN: the length of the probe in the sediment.
N: the number of thermistors used for the calculation of *G*.
G: the temperature gradient calculated by the least square method.
K: the thermal conductivity.
Q: the heat flow value as the product of *G* and *K*.
Stations HF-8 and PC-4 (*) are in the "So-o Trough".

into the sea floor sediment, and calculated by a least square fit of the temperature vs. depth data to a straight line. The probe is 3 m long and 16 mm in diameter, and seven thermistors were installed in it. Because of the shape and material of the lance it is easy to penetrate, but it usually bends when pulled up from the sediment. Therefore it does not allow multiple penetrations. A thermal conductivity was measured on samples taken by the piston coring (PC-3 and PC-4), using the needle probe method (cf. von Herzen and Maxwell, 1959). Samples were laid down on the cabin floor without cutting, taking care not to lose the interstitial water.

The heat flow value is the product of the temperature gradient and the thermal conductivity. Heat flow stations (HF-1 to HF-10) are listed in Table 3 and plotted in Fig. 9b. Stations were aligned from east to west, i.e. perpendicular to the direction of the fault (except for HF-8). The heat flow and topographic cross section along the 35°N parallel (A-A′ in Fig. 9b) is shown in Fig. 10. It is clearly seen that the heat flow distribution has a sharp peak at the topographic inflection, i.e. around the Hatsushima community.

Temperature versus depth profiles are shown in Fig. 11. Measurements from HF-1 to HF-5 were profiles performed during leg 1 of the cruise, and HF-6 to HF-10 during leg 2; their brief descriptions are as follows:

HF-1 was located at the very point where a biological community had been observed. Three of seven thermistors were in the sediment.

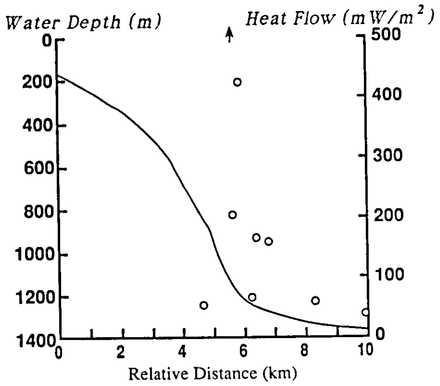

Fig. 10. Heat flow (open circles) and topographic (solid line) cross section along the 35°N parallel (A–A′ in Fig. 9b). Upward arrow is the highest heat flow of 1680 mW/m².

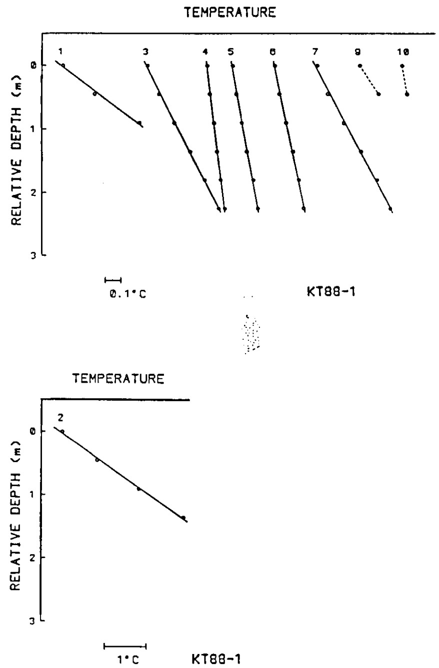

Fig. 11. Temperature versus depth profile of the sediments obtained around the Hatsushima Community.

The temperature gradient was calculated to be 539 mK/m.

HF-2 was situated close to HF-1. Three thermistors were in the mud; the lowermost thermistor was 1.5 meters under the sea floor. The estimated result gave an anomalously high value of 2,130 mK/m. The temperature profile seems convex downward.

HF-3 was on the eastern side of the fault. Six thermistors penetrated, and the profile was straight. The result was 201 mK/m, which is much lower than those obtained at HF-1 and HF-2, but still high compared with other values observed in the vicinity.

HF-4 was located in the basin east of the fault. Six sensors were in the mud, and the profile was straight. The obtained value was rather low (49 mK/m).

HF-5 was located between HF-3 and HF-4. Six thermistors were in the mud, and the profile was again linear. The calculated value was 73 mK/m, lower than HF-3 and higher than HF-4.

HF-6 and HF-7 were located between HF-2 and HF-3. At HF-6, six thermistors penetrated into the bottom and the temperature versus depth profile was linear. The best fit value was 83 mK/m, rather lower than those obtained at surrounding stations. At HF-7, five

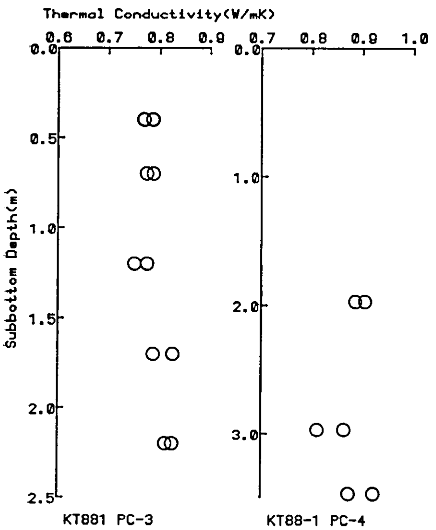

Fig. 12. Plot of thermal conductivity versus depth for PC-3 and PC-4.

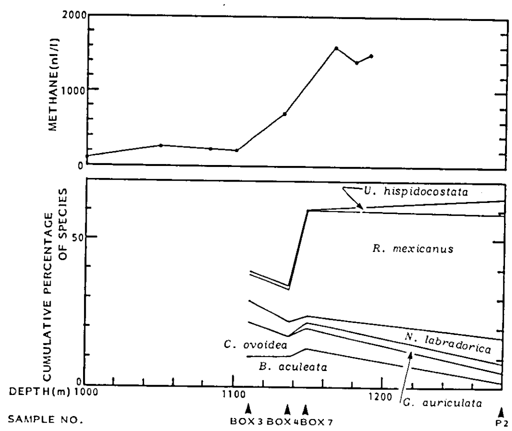

Fig. 13. Depth distributions of 6 major benthic foraminifer species.

thermistors were in the sediment, and the profile was linear. The obtained temperature gradient was 166 mK/m, actually the same as HF-3 close to this site.

HF-8 was the only station located at the eastesn end of Sagami Trough south of the Boso Peninsula. The penetration was not successful, because the wire tension did not change at all when pulled out, and the temperature did not show any significant change.

HF-9 was close to HF-1 and HF-2, where anomalously high heat flow was observed. The bottom state might be coarse, and moreover the probe lance seemed to cause 'buckling'. As a result, the probe tilted without penetration.

HF-10 was located on the slope to the west of other sites. The sea bottom seemed coarse, and although we changed the lance it caused buckling again.

Thermal conductivity was measured for the piston core sample at PC-3, located near HF-1 and HF-2. The obtained thermal conductivity versus depth profile is presented in Fig. 12, showing constant values. Another site PC-4 was at the same point as HF-8 at the eastern end of Sagami Trough.

2-5. Benthic foraminifers

The analyzed samples for benthic foraminiferal assemblage were collected by box corer and piston corer (PC-2) (Fig. 1b). The examined

Table 4. Statistics of the fauna of surface sediments obtained near the Hatsushima Community.

Sample	Plank. foram. No.	Benthic foram. No.	*P/T* ratio	*A/T* ratio
BOX3	68	156	30	4
BOX4	144	157	48	7
BOX7	96	194	33	6
PC-2	92	112	45	2

samples represented the uppermost 1 cm of the collected sediment columns.

About one hundred taxa of the recent benthic foraminifera are identified in the four samples. Figure 13 shows the depth distribution ranges of the main six species (*Bulimina aculeata, Chilostomella ovoidea, Globobulimina auriculata, Nonionellina labradorica, Rutherfordoides mexicanus, Uvigerina hispidocostata*), Table 4 shows planktonic foraminiferal numbers (PEN), benthic foraminiferal numbers (BFN), planktonic foraminifer / total foraminifer ratio (*P/T*) and agglutinated foraminifer / total benthic foraminifer ratio (*A/T*).

The characteristics of foraminiferal distribution are as follows:

1) The species composition of the four samples are obviously different from those at the same depth (1,000 to 1,500 m) of the Northwest Pacific Ocean. Akimoto and Hasegawa (in press) described the distribution of the recent benthic foraminifera around the Japanese Islands. According to them, *B. aculeata, Cassidulina carinata, Melonis parkerae, Pseudoparrella exigua, Uvigerina proboscidea* are dominant in the lower middle bathyal zone in the Kuroshio current region, and *B. aculeata, M. parkerae* and *Uvigerina akitaensis* are predomiunted over the Oyashio current region. However, these species except for *B. aculeata* are minor in the assemblages off Hatsushima Island.

2) The frequencies of the main six species would vary within short distances. Indeed, *R. mexicanus* markedly increases at the sampling sites deeper than 1,140 meters. *G. auriculata, N. labradorica* and *U. hispidocostata* slightly increase downward, but *B. aculeata* and *C. ovoidea* decrease.

3) A relation between the faunal statistics and the water depth was not found in the assemblages off Hatsushima Island. *P/T* ratio and PFN are markedly small in comparison with those at the same water depth in the Northwest Pacific Ocean off southwest Japan.

The characteristics of the distribution lead to the following conclusions: 1) PFN in the surface waters off Hatsushima Island is nearly same as those in other areas of the Northwest Pacific Ocean. This indicates that temperature, salinity and dissolved oxygen in the water column of Sagami Bay are similar to those of other areas of the Northwest Pacific Ocean off the Japanese Islands (AKIMOTO, 1987 MS;

GAMO *et al.*, 1989). AKIMOTO (1987) and GAMO *et al.* (1989) reported the T-S diagram between 1,000 and 1,200 meters water depth off Hatsushima Island. According to them, no spatial fluctuation in temperature is present. The oceanographic data suggest that the sea waters in Sagami Bay are normal.

BFN on the surface of the sediments also resembles those of the Northwest Pacific Ocean. Accordingly, small values of *P/T* ratio and PFN of the examined samples are due to the discussion of planktonic foraminifera in the bottom waters.

2) There is evidence to suggest abnormal condition of the bottom waters. The color of four sediment samples is black. Pyrite grains occur in foraminiferal tests of the samples of Box-cores 7 and PC-2. Methane gas concentrates in the bottom waters (GAMO *et al.*, 1989). Accordingly, the surfaces of sediments are thought to be in an anoxic condition. Such condition would be suggested also by *Calyptogena* in the sample Box-7.

3) In general, the distribution of epifauna, which inhabits the surface sediments, is controlled by the bottom water condition. Under the normal bottom water condition the faunal composition is homogeneous and stable. However, in the study area the frequencies of the main species of the epifauna vary highly from site to site, as shown in Figure 13. Therefore, the bottom water condition locally varies.

4) The faunal change in benthic foraminifera is well correlated with the change in methane concentration (Fig. 13 and Table 4). GAMO *et al.* (1989) pointed out that the high concentration of methan is due to the supply from vent fluids at the *Calyptogena* community site. Accordingly, it is concluded that the abnormal condition of the bottom waters and the relating species composition of benthic foraminifera are formed as result of seepage of methane.

5) Such a peculiar fauna has been reported from sedimentary rocks around the Kuroko ore deposits in the northeast Japan Arc. The Kuroko ore deposits were formed by extrusion of hydrothermal fluid due to submarine volcanism. In fact, high anomaly in temperature ranging from 2.9 to 3.6°C was also detected near the four sites in this study area (GAMO *et al.*, 1989).

6) Small values of *P/T* ratio and PFN off Hatsushima Island may be due to the dissolution of the planktonic foraminifera test in the acid sea water. In fact, OKI (1987 MS) reported that calcium carbonate composed of foraminiferal test dissolves in the acid sea water which is formed by effusion of volcanic gas.

3. Central Sagami Trough

3-1. Submarine topography of the Sagami and the So-o Troughs

Central Sagami Bay is the main sedimentary basin of the Sagami Trough (Fig. 1). Two submarine channels, an axial channel of Sagami Trough and Tokyo canyon, are present, and a large amount of detritus is provided to the Sagami and So-o Troughs. Multichannel seismic profiles suggest that the trough fill sediments of 1.7 sec (two-way travel time) have been deposited since 2 Ma ago (TOKUYAMA *et al.*, 1988). In addition, the Sakawa Fan-delta is developed at the up-dip of the Sagami Trough, which is most likely to be active. A remarkable sedimentary tongue of coarse clastic sediments including gravels with abundant glass and wood fragments was deposited after the Sakawa River flood in July, 1972 (OTSUKA *et al.*, 1974). The axial channels directly connect to this fan-delta; through them passes detritus provided from the Kanto Mountains and adjacent area of Honshu.

The Tokyo submarine fan is a relatively small deep-water cone, 18 km long by 14 km wide, at the mouth of the Tokyo Canyon in 1.2 to 1.6 km water depth (SHEPARD *et al.*, 1964, KAGAMI *et al.*, 1968). The fan is a trench fan on the Sagami Trough, which progrades southwestward to thickly cover the bottom floor of Sagami Trough, then the axis channel gently bends southwestward along the outer margin of the fan. The fan surface is not smooth (cf. KAGAMI *et al.*, 1968), suggesting fan destruction due to erosion and faulting. The bathymetric map shows that the present main feeder channel of the fan is a wide valley which steeply cuts its surface.

The So-o Trough is a southern extension of the Sagami Trough (Fig. 1a). The morphological characteristics around the So-o Trough show that conspicuous northward dipping low angle thrusts are traceable (TAKEUCHI and FUJIOKA 1985; FUJIOKA 1988) along the landward slope of the trough. Small topographic highs forming conical shapes, presumably mud volcanoes (TAKEUCHI and FUJIOKA, 1985), are identified near these thrusts. On the topographic N-S cross sections across the axial channel of the trough, on the seaward slope of the trough a topographic high, which is presumably the outer swell of normal trenches, is recognizable. The axial channel of the trough has a landward dipping smooth surface. Several topographic inflection points are identified on the landward slope which is much steeper than the seaward slope.

Surface sediment features show that the topographic high south of the So-o Trough is also clearly identified, and landward dipping trench wedge structures in the piled bottom sediments and low angle thrust structures on the landward slope are also recognized by a seismic profile obtained during a French-Japanese co-operative study (Kaiko Project) across the So-o Trough (NAKAMURA *et al.*, 1987).

3-2. Description of piston cores

PC-4 Core Description: Axial channel of the Sagami Trough

The PC-4 core (Fig. 2) is composed chiefly of thin-bedded turbidites of *Tbd* and *Tbcd* sequence (BOUMA, 1962), which are approximately 2 cm thick sand layer and 6 cm thick mud layer on averages (Figs. 14 and 15). 10 turbidite layers are identified in the core sample. The burrows (*Scolicial*) are developed mainly in the boundary between the underlying sand and the overlying mud. The sand is composed chiefly of plagioclase, tachylite and sideromelane with small amounts of hornblendes, pyroxenes and biotites. Clinopyroxene and orthopyroxene are identified. Biogenic materials such as nannofossils, diatom and sponge spicules are contained. Foraminifera are likely to be smaller in amount than those of PC-2 and PC-3. The mud is volcanic glass-bearing nannofossil and diatomaceous mud. The presence of hornblende and biotites suggests that the coarse clastic materials are provided not only from the Izu Peninsula side, but also from the Kato Mountains and its adjacent area via the Sakawa and Sagami Rivers.

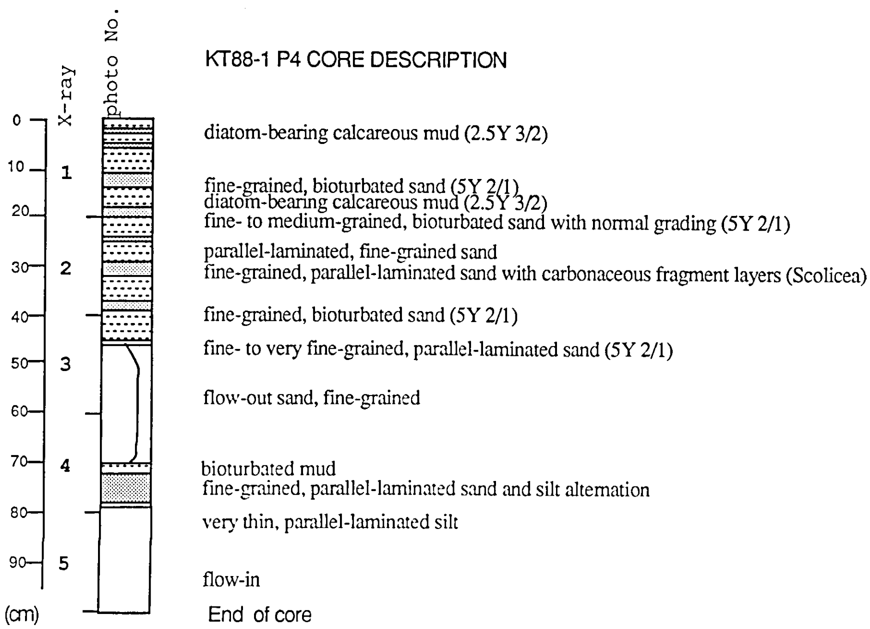

Fig. 14. Piston core log of the PC-4 obtained from So-o Trough.

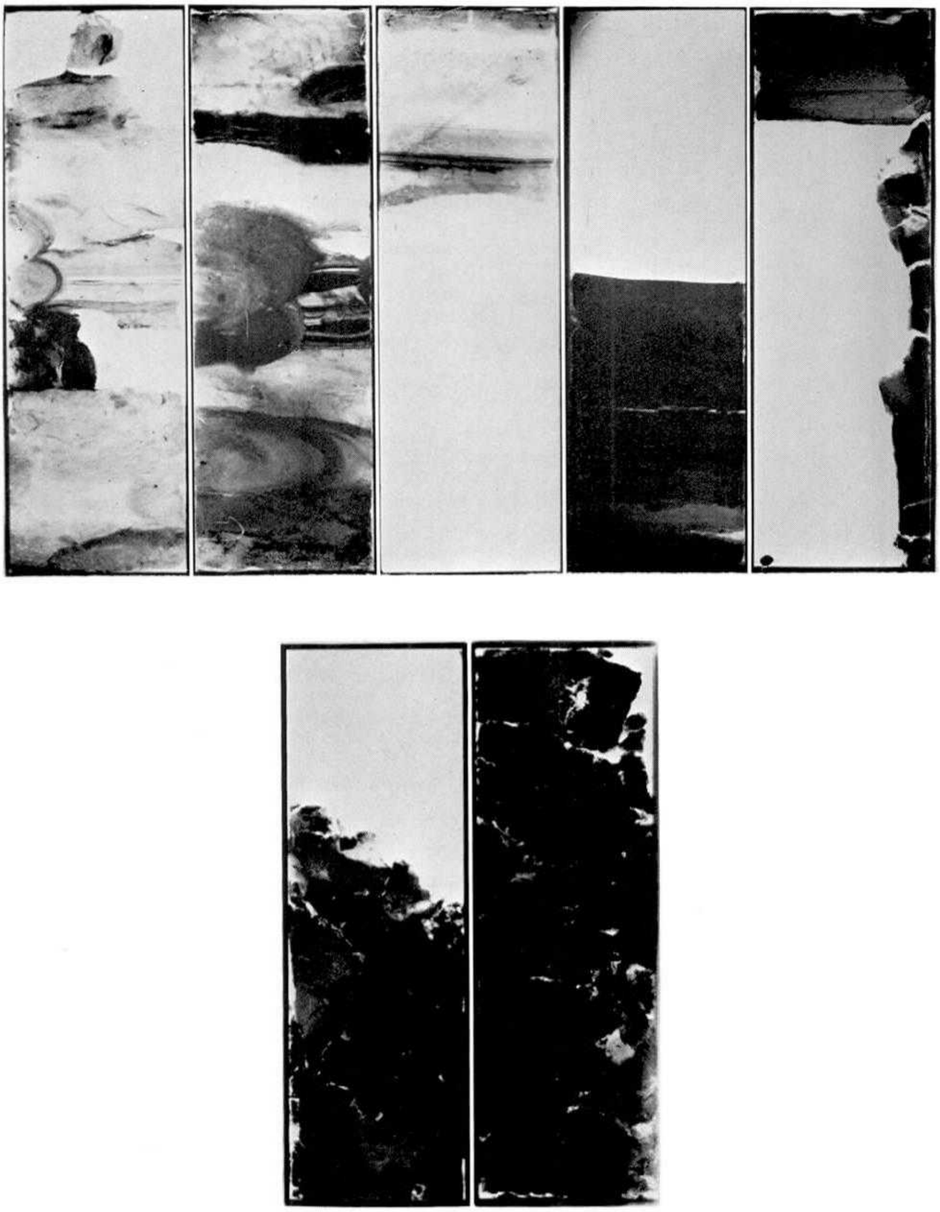

Fig. 15. Soft X-ray photographies of the PC-4 core sample (see Fig. 14. Scale is the same as Fig. 6.

PC-5: Core Description: Western margin of Tokyo Submarine Fan

The PC-5 core sample consists mainly of thin-bedded turbidites consisting of *Tbd* and *Tbc* of Bouma sequence (Figs. 16 and 17). One

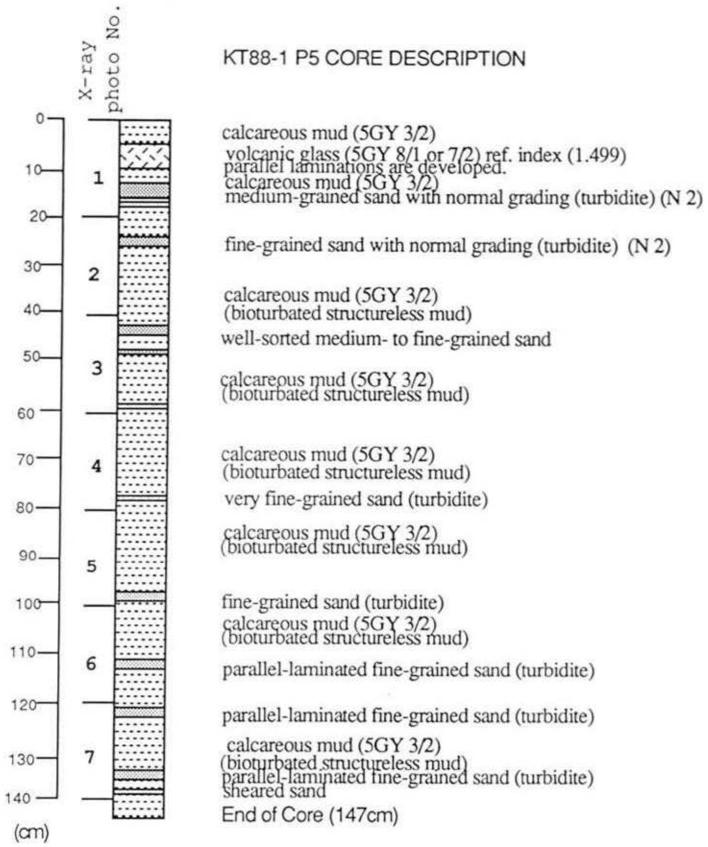

Fig. 16. Piston core log of the PC-5 obtained from the Tokyo submarine fan.

volcanic ash layer is found from 6 cm to 10 cm below the top of the core. 13 turbidite layers are identified in the core sample. The sand layers range from 0.5 cm to 2 cm in thickness, and the muds vary from 4 cm to 20 cm thick. The sand is composed mainly of tachylite, sideromelane, pyroxene and plagioclase. The sand is charaterized by the common presence of hornblende and by that foraminifera tests of this core sample are smaller in amount than those of PC-2 and PC-3 core samples. Noteworthy is that the coarse grained detritus is subrounded or wellrounded, and shows a dirty surface due to abrasion. There are some clay minerals due to alteration, provided probably from the Neogene sequence. Some plagioclase has glass inclusions. The mud is composed of nannofossil and diatomaceous mud with a large amount of plagioclase grains. Tachylite and sideromelane are rare in the mud. Burrows are common, especially from 5 cm to the bottom of the core, but the most sand layers are barely preserved.

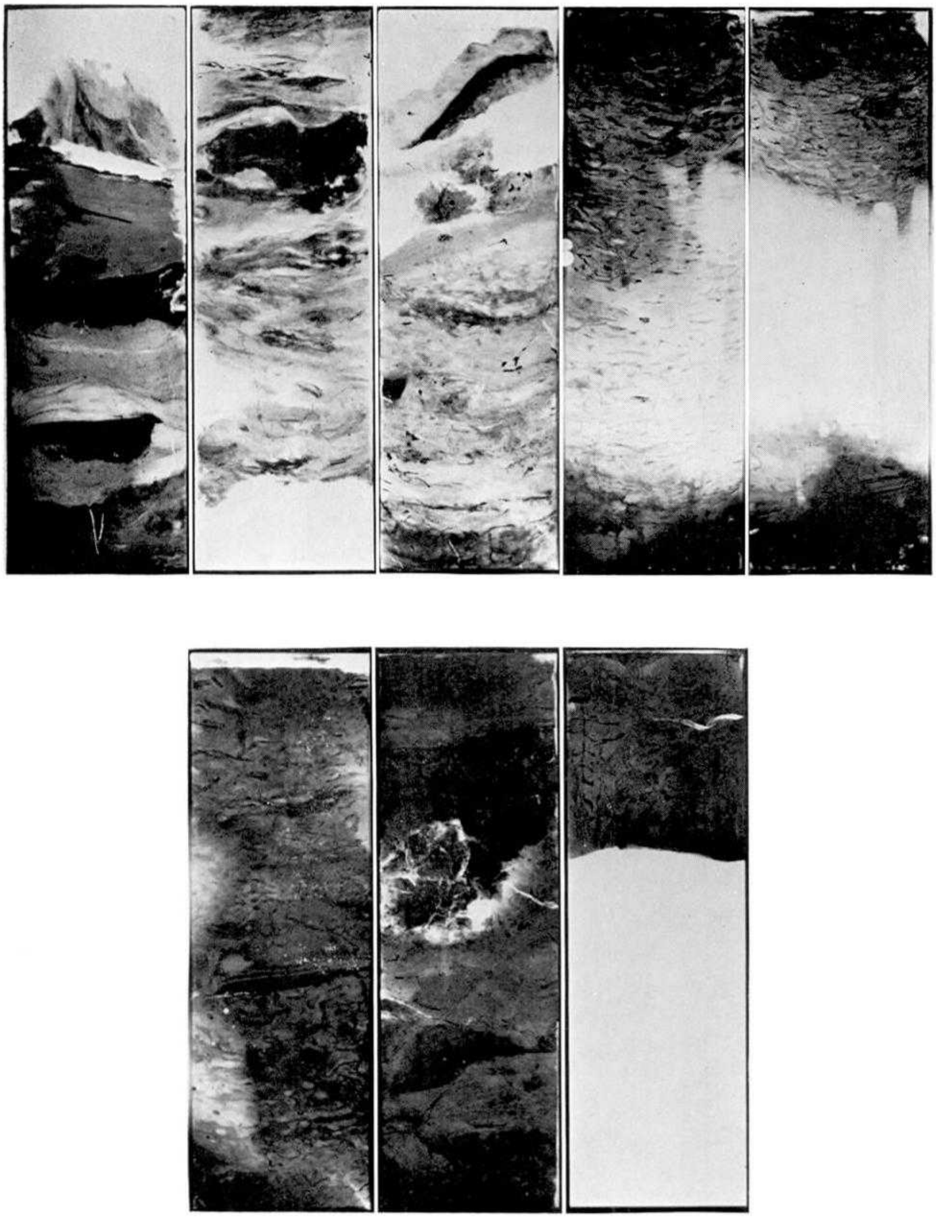

Fig. 17. Soft X-ray photographies of the PC-5 core sample (see Fig. 16. Scale is the same as Fig. 6.

PC-6 Core Description: Western margin of Tokyo Submbrine Fan

The PC-6 core sample is composed of thin-bedded turbidites of *Tbd* and *Tbc* (Figs. 18 and 19). 16 turbidite layers are identified in this core sample. The nature and composition of the materials are quite similar to those of PC-5. The PC-6 is composed mainly of tachylite, sideromelane, pyroxene and plagioclase. Hornblende is also contained. The most particles, especially plagioclase, are subrounded. The detritus grain shows dirty surface, probably due to abrasion. The mud is composed chiefly of nannofossil and diatomaceous mud with

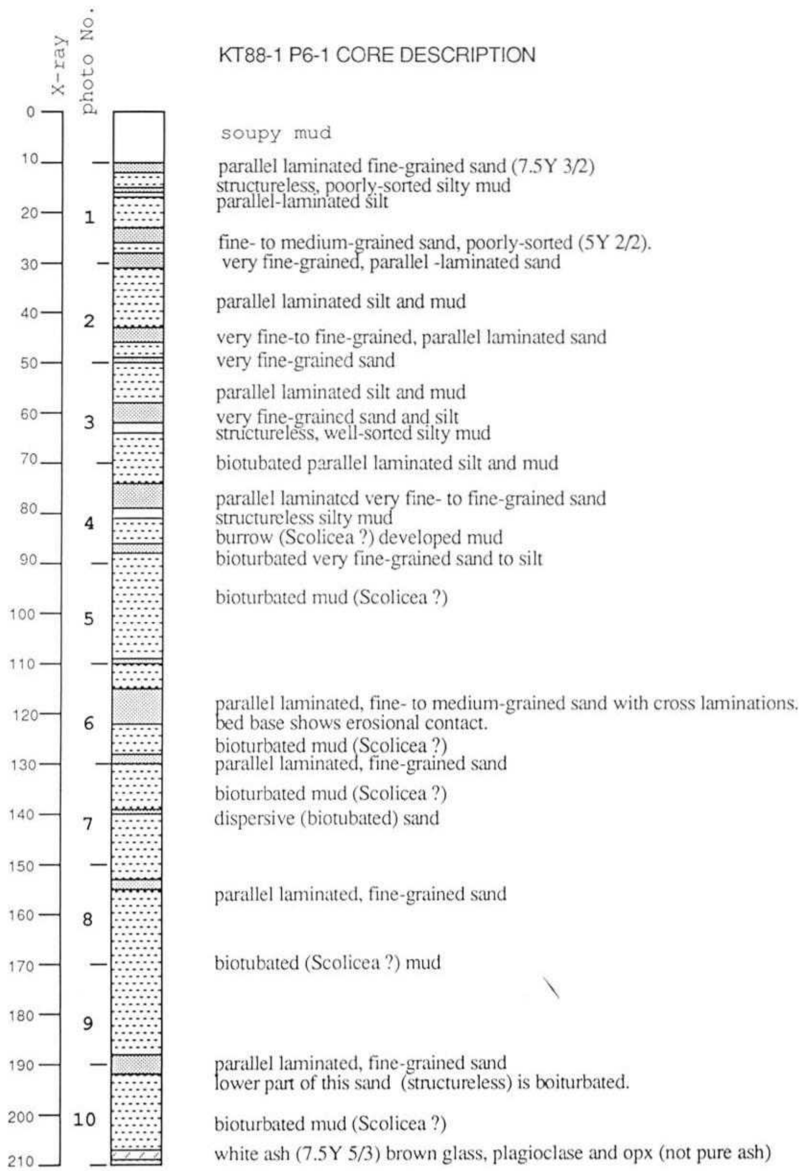

(a)

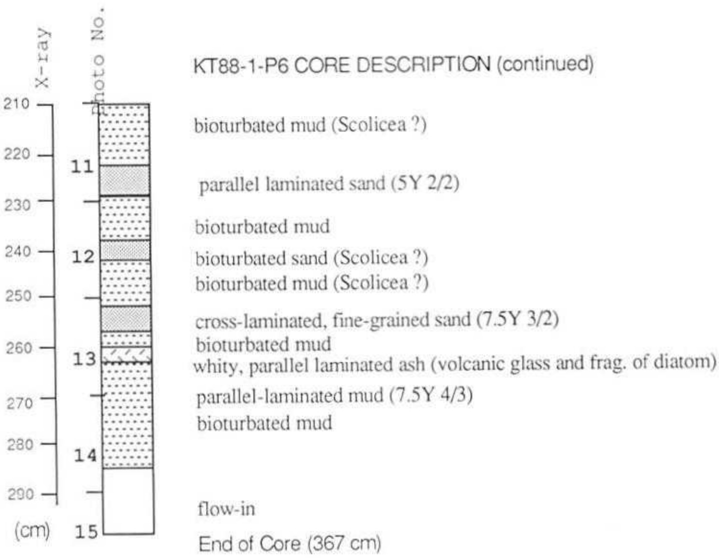

(b)

Fig. 18. Piston core log of the PC-6 obtained from the So-o Trough.

small fragments of plagioclase less than 0.01 mm long.

4. Okinoyama Bank Chain

The Okinoyama Bank Chain NW-SE trending shallow banks occupies the eastern part of Sagami Bay. The banks shows seamount-like shape which consists of various kind of rocks similar to those exposed onland Miura Pensula (KIMURA, 1976; FUJIOKA and FURUTA, 1986). The Okinoyama Bank Chain can be thought to be a manifestation of the Shonan oki submarine volcanoes proposed by MATSUDA (1962). Also, the geological map of the Sagami Bay by KIMURA (1976) draw it as submarine volcanoes on the chain.

4-1. Topography

The Okinoyama Bank Chain has a flat top whose depth is as shallow as 28 meters at the highest peak at the Okinoyama Bank (Fig. 1a). The Okinoyama Bank Chain is cut by east-west trending submarine canyons, one of which is the largest Tokyo Canyon. Summits of the segmented banks are shallower than 500 meters. They seem to be affected by wave base erosion at low sea level stands.

The Okinoyama Bank Chain is called from north to south, the Sagami, the Miura and the Okinoyama Bank.

Just east of the Bank Chain, a small depression called Miura

Basin, which is thickly covered with hemipelagic mud, runs almost parallel to the chain. The depth of the basin is around 600–700 meters. The Okinoyama Bank Chain belongs to the Northeast Japan Plate; the origin of the fault system was thought to be the eduction of the Philippine Sea Plate by NAKAMURA *et al.* (1984).

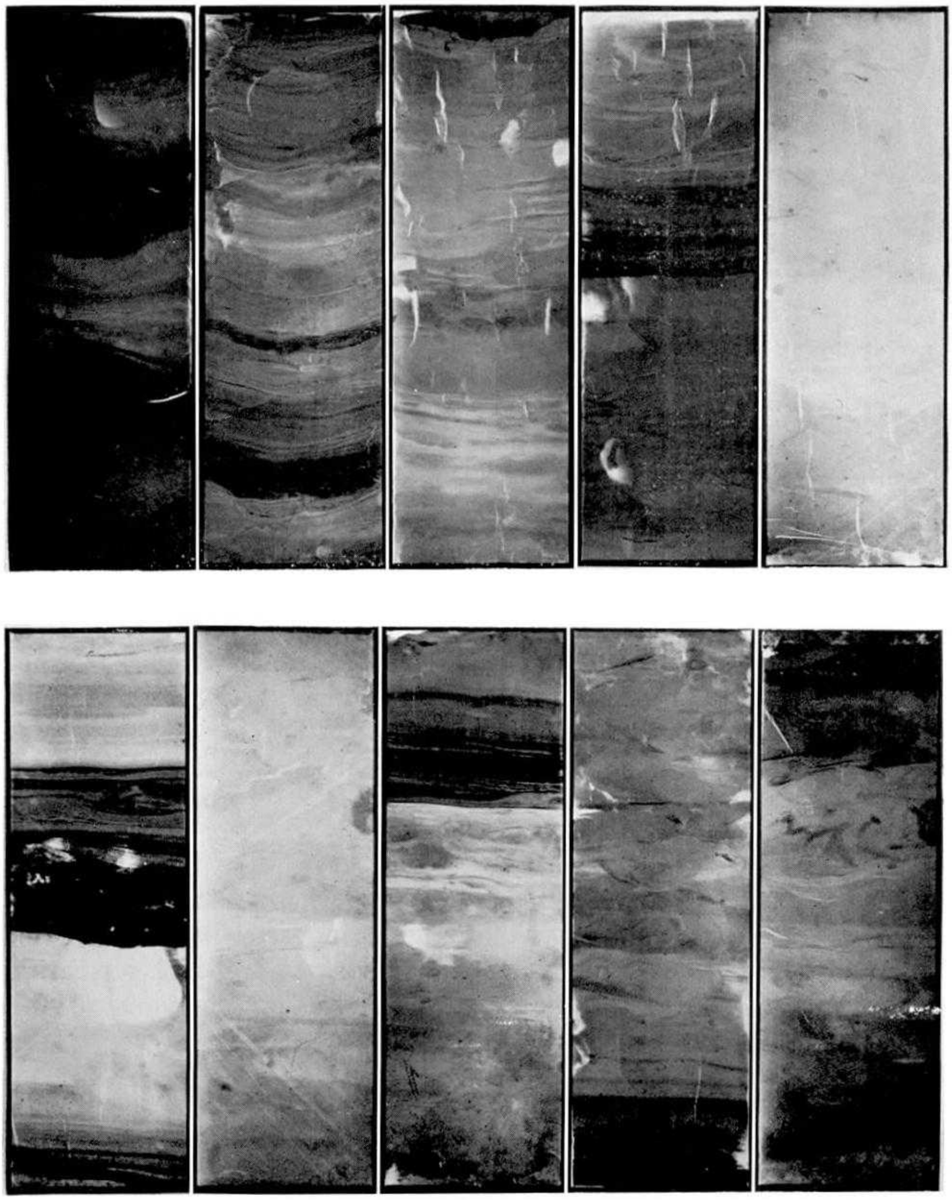

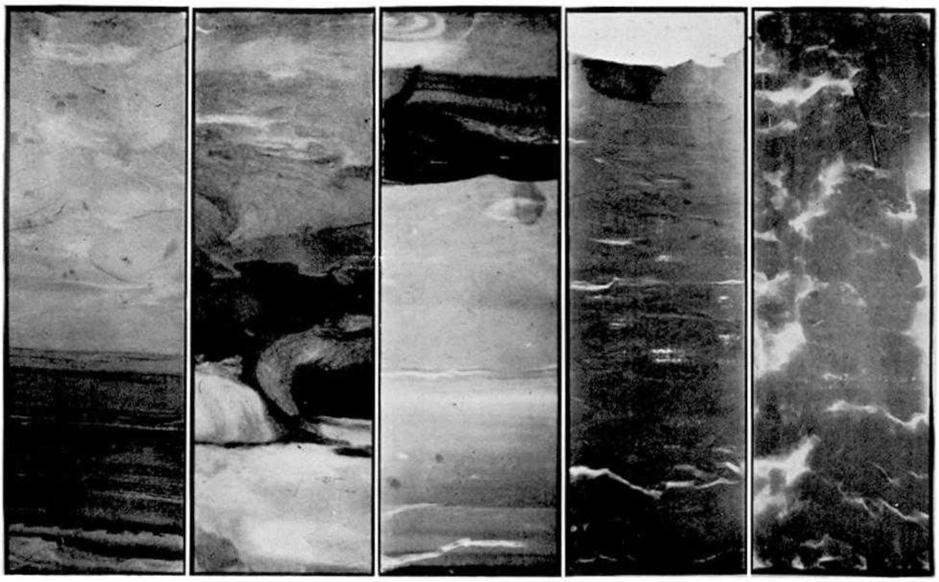

Fig. 19. Soft X-ray photographies of the PC-6 core sample (see Fig. 18. Scale is the same as Fig. 6.

4-2. Major rocks obtained from the Okinoyama Bank Chain

Figure 1b shows the position of the dredge hauls which were recovered during KT88-1 cruise, and Table 5 shows the major lithology of dredged materials. Rocks obtained by the dredge hauls along the Okinoyama Bank Chain are pebbly mudstone or poorly sorted sandstones which are indurated, faulted and fractured dark brown mudstones or sandstones including clasts of volcanic rocks such as basalt, andesite and rhyolite. Volcanic materials are mostly angular in shape.

Volcanics show fluidal and intersertal texture which indicates the typical lava flow origin.

Description of Dredge Samples:

Dredge sampling was performed along the steep flanks of the topographic highs of the Okinoyama Bank Chain and Misaki Bank. Precise positions, depth of each sampling point, and other information are shown in Table 1 and Figure 1b. The samples are composed mainly of unconsolidated and/or semi-consolidated sediments, and some igneous rocks and scoria are identified. Several angular to subangular igneous rocks are found as clasts contained in the unconsolidased or semi-consolidased sediments.

Table 5. List of rocks of the thin sections obtained from samples dredged from the Okinoyama Bank Chain.

Sample	Name	Description
D-1	1	scoria ash
	4	volcanic sand
	5	volcanic sand
	7	v.f. sand
	14	scoria ash
	16	co. ash
	18	volcanis sand
D-2	5	sand
	7	v.f. sand
	9	volcanic sand
	20	sandy tuff
	24	pumiceous tuff
	26	pumiceous tuff
	35	silty sand
D-5	2	volcanic silt
	5	volcanic silt
	18	volcanic silt
	19	volcanic silt
	36	basalt
	78	basalt
D-7	22	volcanic silt
	29	scoria
	83	scoria
	87	scoria
	131	scoria
	163	scoria
D-8	12	volcanic silt
D-10	1	andesite
G-6	8	scoria
G-8	1	basalt
	3	basalt
G-9	1	altered scoria
	7	andesite

Petrographic Study:

A petrographic study was done on six dredge samples and three grab samples of KT88-1 cruise, 14 thin-sections of the unconsolidated and semiconsolidated sediments, 13 thin-sections of the scoria and scoriaceous ash, and six igneous rock thin-sections (Table 5).

Unconsolidated and semi-consolidated sediments are composed mainly of poorly sorted silt with volcanogenic materials. The semi-consolidated sediments commonly suffer weak alteration, and are fractured. Calcite cements and veins are present in the semi-consolidated sediments. However, the fundamental nature and mineral composition of the semi-consolidated and unconsolidated sediments are similar each other. The volcanogenic fragments in the silt, such as fragments of tachylites, plagioclase and pyroxene, are usually angular in shape. Pumice grains are contained, but not common. Some plagioclase grains have glass inclusions (Figs. 20 and 21). Biogenic materials are abundant, including diatoms, sponge spicules, nannofossils and some foraminifera, silicofragellate and carbonaceous fragments. Most of the silt is structureless and poorly sorted, but the preferred orientation of the grains is identified in some sample (*e.g.* D-5-002 and D-5-005).

Most of the volcanic ejecta, scoria and ashes are andesitic or basaltic. The volcanic ejecta occupy about one third of the total amount of

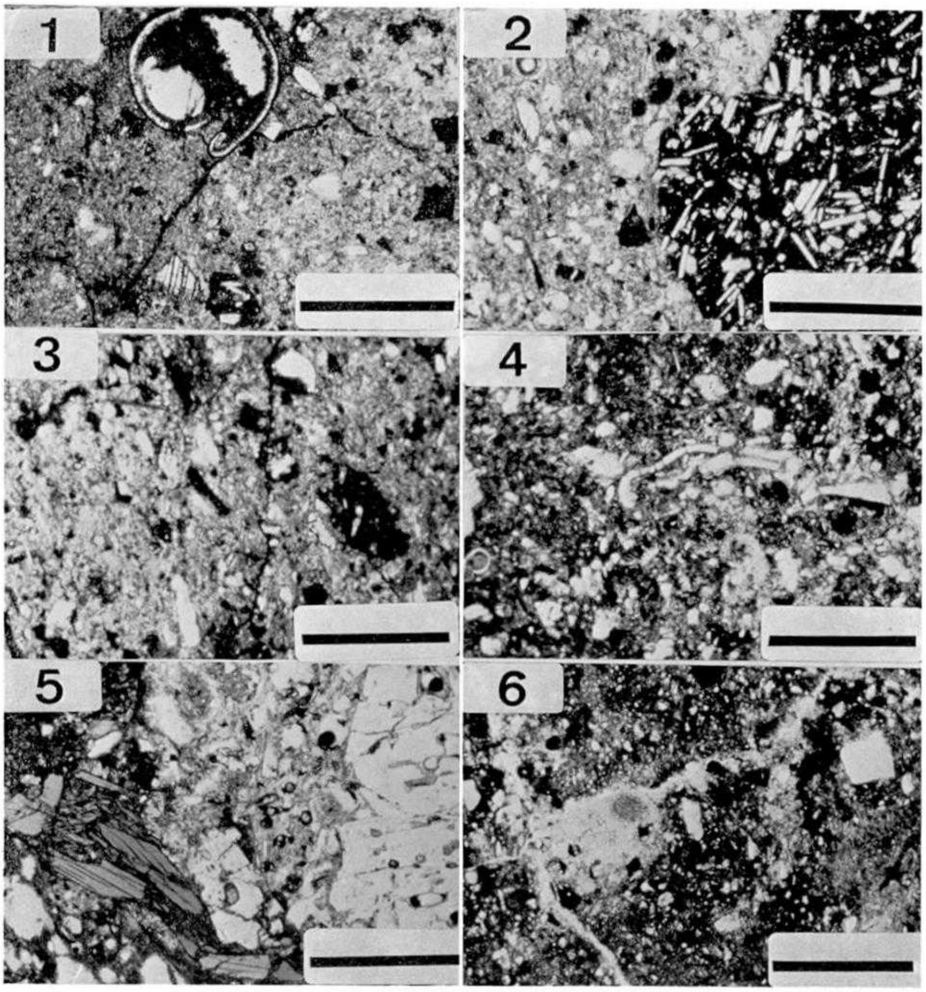

Fig. 20. Photomicrographs of the semicondesolidat volcaniclastic sediments obtained from the Okinoyama Bank Chain. Scale bar is 0.1 mm. 1: D-5 018 open, 2: D-5 005, open, 3: D-5 002, open, 4: D-1 018, open, 5: D-7 029, 6: D-5 019, open.

dredged material. The average grain-size of volcanic ejecta would decreases toward the southeast. D-1 samples are dominated by fine-to coarse-grained ashes without scoria grains. Volcanic ejecta obtained in D-7 are composed chiefly of scoria, more than 2 cm in diameter, and coarse-grained ashes. The scoria in D-7 commonly well-vesiculated, and is composed of fresh tacklite with microlites of plagioclase and pyroxene.

The igneous rock fragments obtained are composed mainly of basalts and andesites. The basalt are dredged from D-5, D-10 and G-8, and andesites are obtained from G-9. The basalt consists of olivine-plagio-

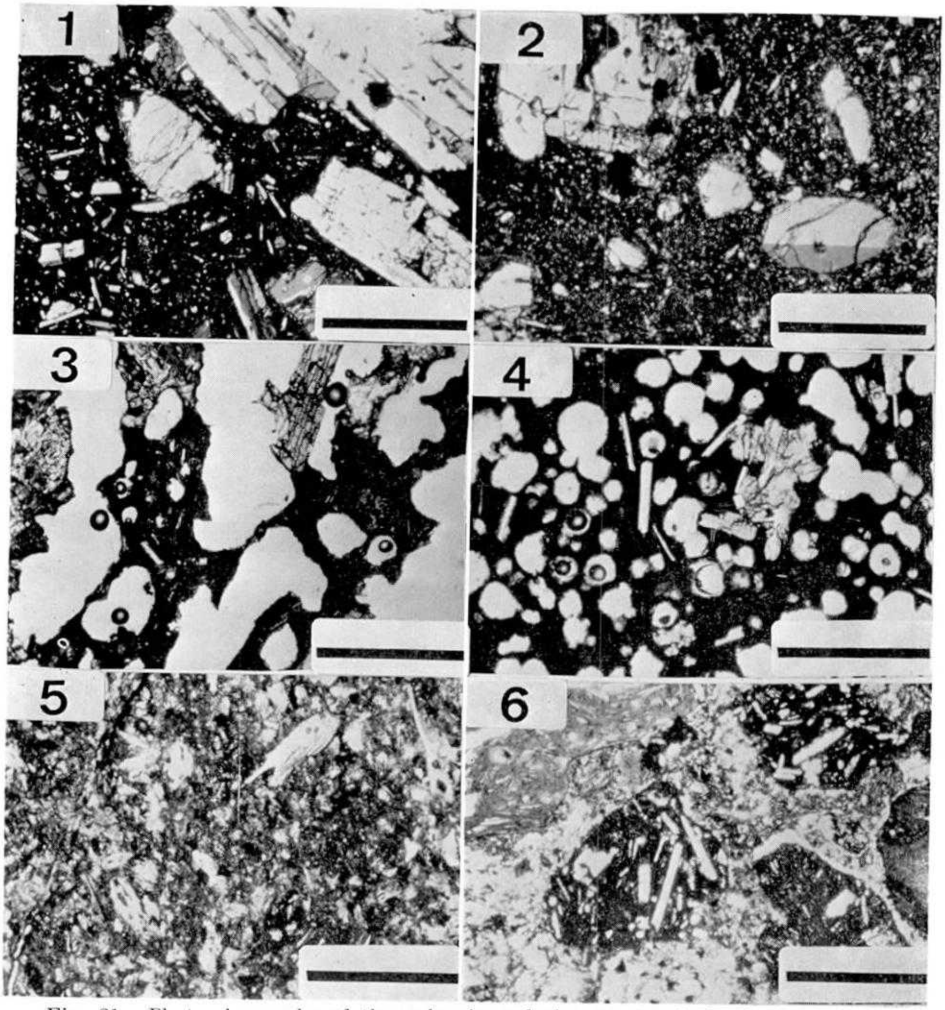

Fig. 21. Photomicrogrphs of the volcanic rock fragments of the dredged samples obtained from the Okinoyama Bank Chain. Scale bar is 0.1 mm. 1: D-5 078, cross, 2: D-10 001, cross, 3: D-7 163, open, 4: G-6 008, open, 5: D-1 016, open, 6: D-2 024, open.

clase basalt of hyalopilitic texture (D-5-036, D-5-078 and D-10-001), and of olivine-bearing basalt of pilotaxitic texture.

4-3. Volcaniclastics

Coarse pebble- to cobble-sized siltstone clasts, semi-consolidated to unconsolidated, were obtained at sites D-1 and D-2 at Okinoyama Bank, D-2 at Okinoyama Bank, D-3, D-4 and D-5 at Misaki Knoll, D-6 at Miura Knoll, D-7, D-8, D-9 and D-10 at Sagami Knoll and G-6, G-8 and G-9 at Senba Spur in Sagami Bay (Figs. 1a and 1b). These siltstone clasts often contain a certain amounts of granules to pebbles of intermediate to basic volcanic rocks. No clasts of plutonic rocks, such as granodiorite, were found. These siltstone clasts are commonly rounded to sub-rounded.

Petrography of Volcaniclastics

At sites of D-1 and D-2 on the southern slope of Okinoyama Bank, pebble to cobble-sized clasts of volcaniclastic conglomerates, volcanic sandstones and pumiceous tuffs were obtained. The conglomerates are composed mainly of rounded to sub-rounded clasts of volcanic rocks, and these clasts are generally clast-supported. They contain a large amount of basalt and andesite clasts up to 3 mm long which exhibit a pronounced poikilitic and/or fluidal texture, and they rarely contain mudstone clasts up to 5 mm long, yielding small amounts of organic remains, such as foraminifers and molluscan shells. The volcanic sandstones show two sorts of different lithofacies. The dominant facies shows that fine to very-fine sized grains, feldspar, quartz and so on, are scattered in the mud matrix. The second facies exhibits medium- to fine-sized grains attached to each other by mud filling interstitials, and this facies is in sharp contact with the former one. The pumiceous tuffs are composed chiefly of very-fine to fine grained glass shards, and they rarely contain a small amounts of marine microfossils.

Clasts of pebble-sized siltstone and basalt were obtained at the site of D-5 on the northeastern slope of the Misaki Knoll. The siltstone clasts contain fine-grained feldspar and mafic minerals, being very angular in shape, and these grains are scattered in the mud matrix. Microfossils are also present in the siltstone. The basalt exhibits a pronounced coarse-grained porphyritic texture.

At sites D-7, 8 and 10 on the southern slope of Sagami Knoll, pebble- to boulder-sized volcaniclastic conglomerates, and pebble-sized siltstones and andesites, were obtained. The volcaniclastic conglomerates consist of mainly scoria clasts, and a small amount of andesite and basalt clasts. These clasts are attached to each other. The interstitials are filled by mud. Plagioclase which occurs as phenocrysts, nearly euhedral and up to 4 mm long, sometimes shows pronounced compositional zoning; a broad, highly calcic core, reaching about An80 in the grain core, surrounded by narrow rims. Some plagioclase phenocrysts have small glass inclusions. Chemical compositions of the inclusions are listed in Table 6.

Chemical Composition of the Volcaniclastics

General Statement and Method of Analysis: In order to classify the clasts of volcanic rocks, chemical analysis was carried out with a Model JCXA-733 electron-probe microanalyzer (EPMA) for SiO_2, TiO_2, Al_2O_3, total iron as FeO, MnO, MgO, CaO, Na_2O, K_2O, Cr_2O_3, V_2O_3, NiO and P_2O_5. The analytical method is as follow: First, the clasts of volcanic rocks are picked up and cleaned with an ultrasonic cleaner, then crushed in an agate bowl. About 100 mg powders are fused to

Table 6-1. Major element chemical compositions of the volcaniclastic materials dredged from the Okinoyama Bank Chain.

1) KT88-1 Volcaniclastics (fused) all list —Bulk—

Sample	G6-8a	G6-8b	D1-30	D5-26a	D5-26b	D6-14a	D6-14b
SiO_2	53.624	50.781	55.727	51.065	51.513	54.936	54.978
TiO_2	1.298	1.175	.982	.800	.663	.728	.752
Al_2O_3	13.778	15.023	14.669	15.137	20.459	19.805	19.034
FeO	12.292	11.620	10.472	8.613	6.742	6.762	2.271
MnO	.223	.195	.308	.178	.116	.146	.165
MgO	5.221	4.751	3.779	4.915	3.777	9.630	2.847
CaO	9.373	9.965	7.950	10.348	12.065	9.278	9.150
Na_2O	2.114	2.242	2.761	2.077	2.115	2.795	2.623
K_2O	.431	.380	.363	.401	.353	.390	.346
Cr_2O_3	0.000	.025	.015	0.000	.033	.018	.017
V_2O_3	.039	.057	.036	.021	.030	.012	.005
NiO	.044	.073	.067	.062	.080	.064	.056
P_2O_5	.048	.098	.082	.058	.064	.080	.066
Na_2O+K_2O	2.545	2.622	3.125	2.478	2.468	3.185	2.069
Total	98.484	96.385	97.211	93.675	98.009	97.642	97.309

Sample	D7-10a	D7-10b	D7-29a	D7-29b	D8-13a	D8-13b	D10-1
SiO_2	50.357	59.254	57.425	53.802	50.314	51.532	53.124
TiO_2	.936	1.011	1.110	1.020	1.065	.991	.819
Al_2O_3	16.785	16.694	14.413	17.507	16.737	18.830	21.555
FeO	8.020	6.653	7.889	7.981	9.715	8.629	7.538
MnO	.164	.121	.164	.124	.224	.136	.144
MgO	2.962	2.082	2.530	3.057	4.032	3.976	2.908
CaO	9.784	7.425	6.635	9.879	8.262	9.278	7.215
Na_2O	3.023	3.755	3.128	3.240	2.517	3.204	3.028
K_2O	.571	.672	.611	.602	.284	.250	.579
Cr_2O_3	0.000	.021	.005	.026	0.000	.021	.011
V_2O_3	.006	.014	.011	.017	.032	.028	.012
NiO	.073	.071	.077	.071	.049	.072	.059
P_2O_5	.023	.112	.064	.047	.074	.082	.162
Na_2O+K_2O	3.594	4.426	3.739	3.838	2.801	3.454	3.608
Total	92.709	97.883	94.066	97.394	93.305	97.029	97.154

Table 6-2

2) KT88-1 Volcaniclastics (fused) all list —Water free—

Sample	G6-8a	G6-8b	D1-30	D5-26a	D5-26b	D6-14a	D6-14b
SiO_2	54.449	56.286	57.326	54.513	52.559	56.262	56.499
TiO_2	1.318	1.219	1.010	.854	.676	.745	.773
Al_2O_3	13.990	15.587	15.090	16.159	20.874	20.283	19.560
FeO	12.481	12.055	10.772	9.194	6.879	6.925	7.472
MnO	.227	.203	.317	.190	.119	.149	.169
MgO	5.302	4.929	3.888	5.247	3.854	2.693	2.926
CaO	9.517	10.339	8.178	11.046	12.311	9.502	9.403
Na_2O	2.146	2.326	2.840	2.218	2.158	2.863	2.695
K_2O	.437	.394	.374	.428	.360	.399	.356
Cr_2O_3	.000	.026	.016	.000	.033	.019	.017
V_2O_3	.040	.059	.037	.022	.031	.012	.006
NiO	.045	.075	.069	.066	.081	.065	.057
P_2O_5	.049	.102	.084	.062	.065	.082	.068
Na_2O+K_2O	2.584	2.721	3.214	2.645	2.518	3.262	3.051
Total	100.000	100.000	100.000	100.000	100.000	100.000	100.000

Sample	D7-10a	D7-10b	D7-29a	D7-29b	D8-13a	D8-13b	D10-1b
SiO_2	54.318	60.535	61.052	55.242	53.925	53.110	54.680
TiO_2	1.010	1.032	1.179	1.047	1.141	1.021	.843
Al_2O_3	18.105	17.055	15.322	17.975	17.938	19.407	22.186
FeO	8.651	6.797	8.387	8.195	10.412	8.893	7.759
MnO	.177	.123	.175	.128	.240	.140	.148
MgO	3.200	2.127	2.690	3.139	4.321	4.098	2.993
CaO	10.553	7.586	7.054	10.143	8.855	9.562	7.426
Na_2O	3.261	3.836	3.325	3.327	2.697	3.302	3.117
K_2O	.616	.686	.649	.618	.304	.258	.596
Cr_2O_3	.000	.022	.005	.027	.000	.022	.011
V_2O_3	.006	.014	.011	.018	.035	.028	.012
NiO	.079	.073	.082	.073	.052	.075	.061
P_2O_5	.024	.114	.068	.049	.079	.084	.167
Na_2O+K_2O	3.877	4.522	3.974	3.941	3.002	3.560	3.713
Total	100.000	100.000	100.000	100.000	100.000	100.000	100.000

be homogenized on an iridium leaf under high voltage. In this method, glassy homogeneous pellets are prepared. The pellets are impregnated with an epoxy resin, then ground and polished with diamond paste. Weight per cents of major elements are then measured by EPMA under the condition that the electron beam is defocused, because the alkali element count decrases with exposure to the beam.

Fourteen volcanic rock fragments were analyzed and are listed in

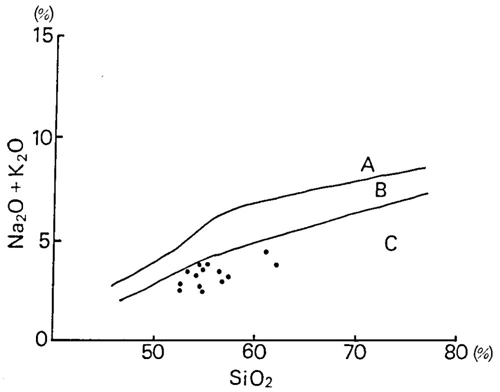

Fig. 22. Silica-alkali diagram for the volcaniclastic rocks of the Okinoyama Bank Chain obtained by dredge hauls. A: Alkali basalt, B: High-alumina basalt, C: Tholeiite.

Table 6. The SiO_2 content of these rocks ranges from 52.6 to 61.1 weight per cent in water-free samples, corresponding to that of basalt to andesite.

$SiO_2-(Na_2O+K_2O)$ Relation

KUNO (1966) proposed the $SiO_2-(Na_2O+K_2O)$ diagram for dividing the volcanic rocks into an alkalic rock series and non-alkalic rock series. Fig. 22 shows the $SiO_2-(Na_2O+K_2O)$ relation of the fragments of volcanic rocks. All the fragments fall in the field of low-alkali tholeiite, suggesting that all volcanic rocks belong to the non-alkalic rock series.

5. Discussion

5-1. Anomalously high heat flow at the Hatsushima Community

Anomalously high heat flow values up to 1,700 mW/m^2 at the Hatsushima Community were obtained during this cruise. Such values have not been observed in Segami Bay so far and are almost equivalent to those of the hydrothermal field such as the Okinawa Trough (YAMANO *et al.*, 1989). Anomalously high CH_4 content of the bottom seawater around the Hatsushima community was also found together with high heat flow anomalies (GAMO *et al.*, 1989). How do we explain these observations in relation to the current tectonics?

Submarine volcanoes called "Higashi Izu-Oki Submarine Volcanoes" lie between the Izu peninsula and Oshima island. The volcanic rocks obtained from these submarine volcanoes are low-alkali tholeiite having olivine phenocrysts and are products of recent submarine eruption (HAMURO *et al.*, 1980).

Active faultings are recognized near or along the topographic inflection line (Research Group of Active Fault, 1980). The prevailing direction of the faults is NNE-SSW, similar to the elongation of the community distribution.

Surface topographic features around the community suggest that they are tectonically extensional. The community site is just on the volcanic front of the Izu-Bonin Arc where high magmatic activities are expected due to subduction of the Pacific Plate underneath the Philippine Sea Plate. These enable us to suggest that the warm, anoxic (hydrothermal) fluid wells up to the seawater/sediment interface resulting in formation of the large community. The benthic foraminifer assemblages observed at the community strongly support this interpretation. This type of deep-sea community is not likely to be the cold seepage type but similar to that of the Mid-oceanic Ridge (FUJIOKA and TAIRA, 1989).

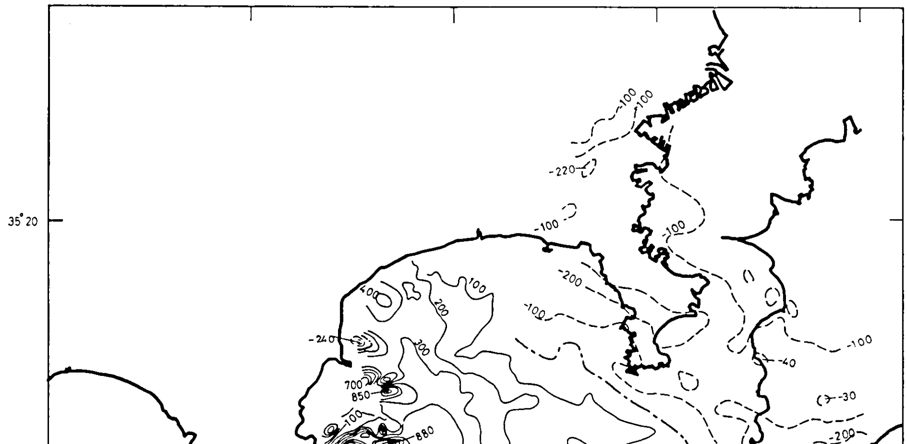

Fig. 23. Geomagnetic anomaly distribution of the geomagnetic total force in Sagami Bay (after UTASHIRO and IWABUCHI, 1971).

5-2. Origin of Okinoyama Bank Chain

Total geomagnetic force anomaly obtained in Sagami Bay was compiled by UTASHIRO and IWABUCHI (1971) (Fig. 23). Many geomagnetic anomalies having a pair of remarkable positive and negative peaks up to about 1,800 nT were recognized around the Oshima island in the NW to SE direction. However, no such definite geomagnetic anomalies (dipoles) have been found along the Okinoyama Bank Chain and magnetic total force value is much lower as compared to that of the Oshima volcano. These mean that the Okinoyama Bank Chain is not composed of volcanoes which show both strong geomagnetic total force and a pair of negative and positive peaks.

KIMURA (1976) showed the volcanic rocks just on the tops of the Okinoyama Bank Chain, and Ito and Masuda (1986) drew submarine volcanoes in the Okinoyama Bank Chain. However, the volcanic rocks were dredged as clasts in the pebble mudstone or as scoria; there is no positive evidence for *in-situ* submarine volcanoes in the Okinoyama Bank Chain. This rejects the possilibility that the Okinoyama Bank Chain was composed of volcanic seamounts. Instead, we propose here the possible accretion of volcaniclastic materials in the Mio-Pliocene mudstone strata.

6. Summary

Results obtained during the cruise of the R/V Tansei-Maru KT88-1 across Sagami Bay are summarized with special references to the Hatsushima Community and the Okinoyama Bank Chain.

(1) Topographic inflection line is clearly observed at water depth of 1,100 meters, east of the Izu peninsula.

(2) Active faults run along the inflection points whose trend is NNE to SSW.

(3) The community site is crossed by the volcanic front of the Izu-Bonin arc.

(4) Various kinds of submarine volcanoes such as Higashi-Izu-oki submarine volcanoes and Atagawa-oki submarine lava flow are identified.

(5) High heat flow and high methane anomalies were observed at the Hatsushima Community.

(6) These observations strongly suggest that submarine hot springs sustain the deep sea community of the Hatsushima area.

(7) Both weak magnetic total force and lack of a pair of positive and negative anomalies show the non-existence of submarine volcanoes around the Okinoyama Bank Chain.

(8) Dredged materials show the possible accretion of volcaniclastic

materials in the Miocene to Pliocene mudstone strata.

Acknowledgments

During KT88-1 cruise, Captain Igarashi and all the crew of the R/V Tansei-maru helped us with station surveys. They helped with dredge hauls, deep sea cameras, heat flow and so on. They are acknowledged. Thanks are also due to Drs. T. Furuta, Ocean Research Institute, B. -C. Suk, Ocean Research Institute, Korea and M. Ito, Chiba University, and Mrs. T. Yamagata, Kyusyu University and J. Ando, Tohoku University, for their valuable suggestions and help during the cruise. During the preparation of the manuscript, Drs. T. Gamo, Ocean Research Institute, S. Uyeda, Earthquake Research Institute and K. Otsuki, Tohoku University gave us valuable comments. Mr. P. Blume, Kyoto University critically read the manuscript. Mr. Kinzo Yoshida, Mrs. T. Kanahara, Ms. A. Yasue and Ms. N. Yasuzato helped with preparing may thin-sections, typing and drawing.

References

AKIMOTO, K., 1987MS, Paleoenvironmental studies of the Nishiyatsushiro and Shizukawa Groups, South Fossa-Magna Region. Tohoku Univ., Doctoral Dissertation.

AKIMOTO, K. and S. HASEGAWA, in press, Bathymetric distribution of the recent benthic foraminifers around Japan. —as a contribution to the new paleobathymetric scale—. *Mem. Geol. Soc. Japan*, **32**.

BOUMA, A. H., 1962, Sedimentology of some flysch deposits—a graphic approach to facies interpretation, 168p., Elsevier Pub. Co., Amsterdam.

FUJIOKA, K,, 1988, Topographic features around Izu Oshima Island, *Jour. Geography*, **97**, 39-50, (in Japanese with English abstract).

FUJIOKA, K. *et al*, 1984, Geology of the Boso Submarine Escarpment, southeast of Tokyo—preliminary report of the Tansei Maru Cruise KT83-20, *Bull. Earthq. Res. Inst., Univ. Tokyo*, **59**, 267-326.

FUJIOKA, K. and T. FURUTA, 1986, Topography and structure of the Okinoyama bank chain-results of observations from the Shinkai 2000 around the Miura knoll-, *JAMSTEC Deepsea Res.*, **2**, 1-9.

FUJIOKA, K. and A. TAIRA, 1989, Tectono-sedimentary settings of seep biological communites —a syntheses from the Japanese subduction zones—. In A. Taira and F. Masuda eds. *Sedimentary Facies in the Active Plate Margin*, Terra Sci. Pub. Co., Tokyo, 577-602.

GAMO, T., J. ISHIBASHI, K. SHITASHIMA, M. KINOSHITA, M. WATANABE, E. NAKAYAMA, Y. SOHRIN, W. -S. KIM., T. MASUZAWA and K. FUJIOKA, 1989, Anomalies of bottom CH_4 and trace metal concentrations associated with high heat flow at the *Calyptogena* community off Hatsu-shima Island, Sagami Bay, Japan: A preliminary report of Tansei Maru KT-88-1 cruise Leg-1.

HAMURO, K., S. ARAMAKI, H. KAGAMI and K. FUJIOKA, 1980, The Higashi-Izu-oki submarine volcanoes, part 1. *Bull Earthq. Res. Inst., Univ. Tokyo*, **55**, 259-298 (in Japanese with English abstract).

HASHIMOTO, J., T. TANAKA, S. MATSUZAWA and H. HOTTA, 1987, Surveys of the deep-sea communities dominated by the giant clam, *Calyptogena soyae*, along the slope foot of

Hatsushima Island, Sagami Bay, *JAMSTEC Deepsea Res.*, **3**, 37–47 (in Japanese with English abstract).

ISHIBASHI, K., 1976, Interpretation of abnormal uplifling around Izu Peninsula and 'Izu-Toho Line-west Sagami Bay Fault', multisubduction in boundary of the northmost Philippine-Sea Plate, *Abst. Earthq. Soc. Japan*, **2**, 29.

ITO, M. and F. MASUDA, 1986, Evolution of clastic piles in an arc-arc collision zone: Late Cenozoic depositional history around the Tanzawa Mountains, central Honshu, Japan. *Sediment. Geol.*, **49**, 223–259.

KAGAMI, H., E. HONZA, M. KIMURA, M. INOUE and N. NASU, 1968, Minimisagami Formation in Sagami Trough. *Jour. Mar. Geol.*, **4**, 1–15 (in Japanese with English abstract).

KANAMORI, H, 1971, Faulting of the Great Kanto Earthquake of 1923 as revealed by seismological data. *Bull. Earthq. Res. Inst.*, **49**, 13–18.

KIMURA, M. 1976, Marine geology in the Sagami-nada Sea and its vicinity. *Marine Geol. Map ser.* **3**, Geol. Surv. Japan, 10p.

KUNO, H. 1966, Lateral variation of basalt magma type across continental margins and island arcs, *Bull. Volcanologique*, Ser. II, **27**, 195–222.

MATOBA, Y., 1970, Distribution of recent shallow water foraminifera of Matsushima Bay, Miyagi Prefecture, northeast Japan. *Sci. Rep., Tohoku Univ.*, 2nd ser., **42**, 1–85.

MATSUDA, T., 1962, Crustal deformation and igneous activity in the south Fossa Magna, Japan. *Amer. Geophys. Union, Monogr.*, **6**, 140–150.

NAKA, J., T. TANAKA and H. HOTTA, 1988, A submarine Lava Flow in the Western Part of the Sagami Bay, northeast off Atagawa (II). *JAMSTEC Deepsea Research* **4**, 15–176.

NAKAMURA, K., K. SHIMAZAKI and N. YONEKURA, 1984, Subduction, bending and eduction-Present and Quaternary tectonics of the northern border of the Philippine Sea plate. *Bull. Soc. Geol. Frn.* **26**, 221–243.

NAKAMURA, K. *et al.*, 1987, Oblique and near collision subduction, Sagami and Suruga Troughs—preliminary results of the French-Japanese 1984 Kaiko cruise, Leg 2. *Earth and Planet. Sci. Lett.*, **83**, 229–242.

OHTA, S., H. SAKAI, A. TAIRA, K. OHWADA, T. ISHII, M. MAEDA, K. FUJIOKA, T. SAINO, K. KOGURE, T. GAMO, Y. SHIRAYAMA, T. FURUTA, T. ISHIZUKA, K. ENDOW, T. SUMI, H. HOTTA, J. HASHIMOTO, N. HANDA, T. MATSUZAWA and M. HORIKOSHI, 1987, Report on multi-disciplinary investigations of the *Calyptogena* communities at the Hatsushima site. *JAMSTEC Deepsea Res.*, **3**, 51–60 (in Japanese with English abstract).

OKI, K., 1987MS, Echological analysis of the dead and living assemblages of benthonic foraminifera in Kagoshima Bay, South Kyushu, Japan. Tohoku Univ. Doctoral Dissertation.

OTSUKA, K., H. KAGAMI, E. HONZA and N. NASU, 1974, Submarine slumping as a cause of turbidity currents in the Sagami Bay. *Kaiyo Kagaku (Mar. Sci.)*, **5**, 446–452 (in Japanese).

SAKAI, H., T. GAMO, K. ENDO, J. ISHIBASHI, F. YANAGISAWA, M. KUSAKABE, T. AKAGI, T. ISHIZUKA, G. IGARASHI and S. OHTA, 1987, *Calyptogena* colonies on the seabed off Hatsushima, Sagami Bay, A geological study with SHINKAI 2000. *JAMSTEC Deepsea Research* special issue, 75–90 (in Japanese with English abstract).

SHEPARD, F. P., H. NIINO and T. K. CHAMBERLAIN, 1964, Submarine canyons and Sagami Trough, east-central Honshu, Japan. *Bull. Geol. Soc. America*, **75**, 1117–1130.

SUGIMURA, A., 1972, Plate boundaries around Japan and its environs. *Kagaku*, **42**, 192–202 (in Japanese).

TADA, T. and M. HASHIMOTO, 1988, *Programme and Abstracts, The Seismological Soc. of Japan*, 1988, No. 1, B55.

TAKEUCHI, A. and K. FUJIOKA, 1985, Submarine geomorphology along the Sagami and Suruga Troughs. *Jour. Geography*, **94**, 102–114 (in Japanese with English abstract).

TOKUYAMA, H., K. SUYEHIRO, H. WATANABE, M. OHNISHI, A. TAKAHASHI, T. IKAWA, M.

ASADA, K. FUJIOKA, J. ASHI, S. KURAMOTO, W. SOH and Y. OGAWA, 1988, Multichannel seismic reflection profile from south of the Izu Oshima. *J. Volcanol. Soc. Japan* **33**, 67-77 (in Japanese with English abstract).

UI, T., S. ARAMAKI and Y. MIYAKE, 1988, Subaqueous basaltic lava flow at the Sagami Bay. *JAMSTEC Deepsea Res.* **4**, 149-156, 1988.

UTASHIRO, S. and Y. IWABUCHI, 1971, The submarine topography and geological structure of Sagami Bay, south coast of Honshu, Japan. *Jour. Geogr.*, **80**, 77-80 (in Japanese with English).

Von HERZEN, R. P. and A. E. MAXWELL, 1959, The measurement of chermal conductivity of deep-sea sediments by a needle-probe method. *J. Geophys. Res.*, **64**, 1557-1563.

WALTON, W. R., 1952, Tequniques for recognition of living foraminifera. *Contr. Cushman Found. Foram. Res.*, **3**, 56-60.

YAMANO, M., S. UYEDA, J. P. FOUCHER and J. C. SIBUET, 1989, Heat flow anomaly in the middle Okinawa Trough, *Tectonophysics*, **159**, 307-318.

相模湾とその周辺の地質

——KT88-1 次航海報告——

藤岡換太郎[1]・木下正高[2]・徐　垣[1]・塚脇真二[1]
芦寿一郎[1]・秋本和実[2]・渡辺正晴[1]

[1] 東京大学海洋研究所
[2] 東京大学地震研究所

1988 年 2 月相模湾の地質・地球物理・地球化学等の総合的な調査が東京大学海洋研究所の淡青丸によって行なわれた．日本列島周辺で最大の深海生物群集である相模湾西部の初島の南にある初島生物群集では最高 1680 mW/m^2 に達する高地殻熱流量の異常が観察された．それとともにメタン (CH_4) の高異常を示す海底直上の海水が得られた．これらの結果は初島生物群集の立地について新しいアイディアを提出させることになった．初島生物群集周辺の地形，表層堆積物，堆積物中の底生有孔虫の結果や地球物理・地球化学的性質は，初島生物群集が地下のマグマに関係した海底温泉によって形成されている可能性を強く示唆している．

相模湾の東部にあり北西-南東方向の配列をしている浅瀬，沖ノ山堆列では地形と地質の調査が行なわれ，火山性堆積物を含む大量の泥岩がドレッジによって得られている．従来海上保安庁水路部により提出されている地磁気異常と全磁力の分布とから沖ノ山堆は火山の列ではなく，中新世から鮮新世にかけての火山フロント近くから供給された火山性物質が陸側斜面に付加してできた可能性が高い．